Journal of
Materials Chemistry C

Accepted Manuscript

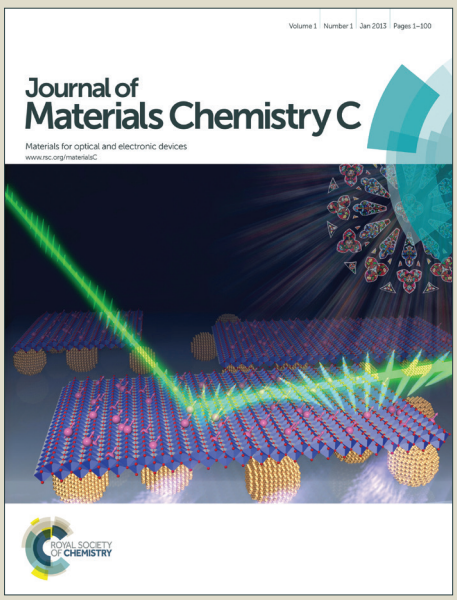

ROYAL SOCIETY OF CHEMISTRY

www.rsc.org/materialsC

Journal of Materials Chemistry C
CREATED USING THE RSC ARTICLE TEMPLATE (VER. 2.1) - SEE WWW.RSC.ORG/ELECTRONICFILES FOR DETAILS

o-Carborane derivatives for probing molecular polarity effects on liquid crystal phase stability and dielectric behavior†

Jacek Pecyna,[a,b] Aleksandra Jankowiak,[a] Damian Pociecha,[c] and Piotr Kaszyński*[a,b,d,e]

Receipt/Acceptance Data **[DO NOT ALTER/DELETE THIS TEXT]**
Publication data **[DO NOT ALTER/DELETE THIS TEXT]**
DOI: 10.1039/b000000x [DO NOT ALTER/DELETE THIS TEXT]

A series of mesogenic derivatives of *o*-carborane was synthesized, their properties were analyzed by thermal, optical and XRD methods, and results were compared with those of isostructural *p*-carborane and benzene analogues. Comparative analysis revealed lower nematic phase stability and enhanced smectic behavior, including SmC, in the *o*-carborane derivatives relative to the isosteric *p*-carborane analogues. The effect of *o*-carborane on electrooptical properties was assessed for biphenyl derivative **1[B]a** in **6CHBT** nematic host giving the extrapolated Δε = 11.0, and a moderate increase of elastic constants K_{ii}. Complete analysis of dielectric results for *o*-carborane and *p*-carborane analogues **1[B]a** and **1[A]a** with the Maier-Meier formalism was augmented with DFT computational methods.

Introduction

During the past two decades *para*-carborane,[1] [*closo*-1,12-$C_2B_{10}H_{12}$] (**A**, Fig. 1), has become an attractive linear structural element of liquid crystals,[2-4] molecular construction sets,[5,6] and pharmacological compounds,[7-9] owing primarily to its geometry, symmetry, and chemical reactivity. In contrast, the two isomers of **A**, *ortho*-carborane (**B**) and *meta*-carborane (**C**) received much less attention, even though they have additional properties that are of particular interest for certain molecular and functional designs. For instance, in contrast to **A**, *ortho*- and *meta*-carboranes have ground-state dipole moments of 4.53 D and 2.85 D, respectively,[10,11] which are oriented about 30° to the 1,12-axis for **B** and nearly parallel to the 2,9- axis in **C** (Fig. 1). The different magnitude and orientation of the molecular dipole moment in the three essentially isosteric carboranes are of interest for fundamental studies of the liquid crystal phenomenon and for developing of materials for LCD applications.[12,13] One such a fundamental question relates to the role of the molecular electric dipole in smectic phase induction and liquid crystalline phase stabilization in general.[14,15] A comparison of properties of isosteric mesogenic derivatives **IA** – **IC** would provide an opportunity for such investigation, and also for the development of new polar materials for electrooptical applications.

Recently, we have reported practical access to isomerically pure 1,12-difunctionalized derivatives of *o*-carborane,[16] which opened up the door to investigation of new classes of liquid crystals of type **IB**. In this context two such derivatives, **1[B]a** and **2[B]e** (Fig. 2) were prepared and their preliminary studies indicated a significant smectogenic character,[16] which warrants further detailed investigation. Here we describe synthesis and characterization of a series of isostructural derivatives **1** and **2** (Fig. 2) in which isosteric carborane derivatives of type **IA** and **IB** are compared to those of benzene analogues. The smectic phases are analyzed by powder XRD and selected derivatives are investigated by dielectric methods as low concentration

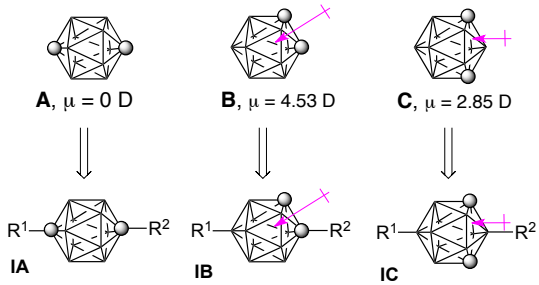

Fig 1. The structures of three isomeric carboranes [*closo*-$C_2B_{10}H_{12}$], **A**, **B** and **C**, and their disubstituted derivatives **IA**, **IB**, and **IC**, respectively. Each vertex represents a BH fragment and the sphere is a carbon atom. The arrow represents the electric dipole vector of the cluster (values from ref [10]).

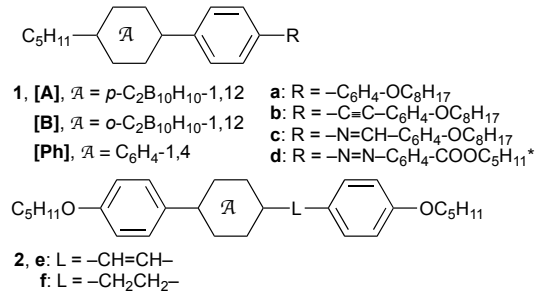

Fig. 2. The structures of investigated compounds. Definitions of rings **A** and **B** are shown in Fig. 1.

[a] *Department of Chemistry, Vanderbilt University, Nashville, TN 37235, USA, Tel: 1-615-322-3458; E-mail: piotr.kaszynski@vanderbilt.edu.*
[b] *Department of Chemistry, Middle Tennessee State University, Murfreesboro, TN 37132, USA.*
[c] *Department of Chemistry, University of Warsaw, Zwirki i Wigury 101, 02-089 Warsaw, Poland.*
[d] *Faculty of Chemistry, University of Łódź, Tamka 12, 91-403 Łódź, Poland.*
[e] *Centre of Molecular and Macromolecular Studies, Polish Academy of Sciences, Sienkiewicza 112, 90-363 Łódź, Poland.*

† Electronic Supplementary Information (ESI) available: details of thermal and dielectic analysis of binary mixture, additional XRD data, partial results of DFT calculations, archive of equilibrium geometries for **1[A]a** and **1[B]a**. This material is available free of charge via the Internet at http://pubs.acs.org. See http://dx.doi.org/10.1039/b000000x/

additives in a nematic host. Experimental results are augmented with DFT calculations and dielectric data are analyzed by the Maier-Meier formalism.

Results

Synthesis

Biphenyls **1a** were obtained from appropriate haloarenes **3** in C–C cross-coupling reactions with 4-$C_8H_{17}OC_6H_4M$ (Scheme 1): Suzuki for **1[A]a** (Hal = Br,[17] M = $B(OCH_2)_2$),[18] Negishi for **1[B]a** (Hal = I, M = ZnCl),[16] and Kumada for **1[Ph]a** (Hal = I,[19] M = MgBr),[18] and their details are described elsewhere. The iodoarenes **3** (Hal = I) were also used for a modified Sonogashira[20] coupling reaction with 4-$C_8H_{17}OC_6H_4CCH$[21,22] and preparation of tolanes **1b** (Scheme 1); the corresponding bromides were ineffective in this reaction. The reaction was conducted at ambient temperature in the presence of anhydrous non-nucleophilic Hunig's base to avoid amine- and hydroxide-promoted deboronation of *o*-carborane derivatives.

Anilines **4[A]**, **4[B]**,[16] and **4[Ph]** [5] served as suitable precursors to Schiff bases **1c** and azobenzene derivatives **1d** obtained by acid-catalyzed condensation with 4-$C_8H_{17}OC_6H_4CHO$ and 4-nitrosobenzoate ester **5**, respectively (Scheme 1). Aniline **4[B]** was also converted to the corresponding iodide **3[B]** (Hal = I) by a modified Sandmeyer reaction,[16] while iodide **3[A]** (Hal = I) was obtained by transhalogenation of the analogous bromide[17] **3[A]** (Hal = Br, *n*-BuLi followed by I_2).

SCHEME 1

Dimethylene-linked derivatives **2f** were obtained by Pd-catalyzed hydrogenation[23] of the previously reported stilbenes **2e**,[16,23] as shown for **2[B]f** in Scheme 2.

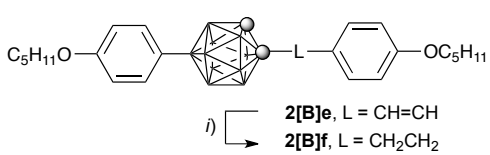

Scheme 2. Synthesis of liquid crystal **2[B]f**. Reagents and conditions: *i*) H_2 (50 psi), Pd/C (10%), THF, rt.

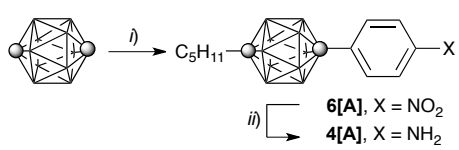

Scheme 3. Synthesis of aniline **4[A]**. Reagents and conditions: *i*) 1. *n*-BuLi, THF, –78 °C→0 °C; 2. *n*-$C_5H_{11}I$, –78 °C→rt; 3. DME, *n*-BuLi, –78 °C→rt; 4. CuI, 0 °C; 5. Pyridine; 6. 4-$IC_6H_4NO_2$, reflux; *ii*) H_2 (40 psi), Pd/C (10%), THF, rt.

The preparation of aniline derivative of *p*-carborane **4[A]** is shown in Scheme 3. The first step is a one-pot alkylation–arylation[24] process, which gave the desired nitrophenyl derivative **6[A]** in 20% yield after careful chromatographic separation from several by-products. Subsequent catalytic reduction of **6[A]**, as described for **6[B]**,[16] gave aniline **4[A]**.

The nitroso ester **5** was prepared by partial oxidation of the known[25,26] 4-aminobenzoate ester **7** with Oxone®, according to a general literature procedure[27] (Scheme 4).

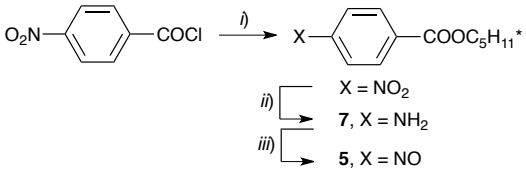

Scheme 4. Synthesis of nitroso ester **5**. Reagents and conditions: *i*) (*S*)-2-methylbutan-1-ol, pyridine; *ii*) H_2 (40 psi), Pd/C (10%), THF, rt; *iii*) Oxone®, CH_2Cl_2/H_2O, rt.

Thermal analysis

Transition temperatures and enthalpies of compounds **1** and **2** were determined by differential scanning calorimetry (DSC). Phase structures were assigned by optical microscopy in polarized light and confirmed by powder XRD measurements. The results are shown in Tables 1 and 2 and Fig. 3–5.

All carborane derivatives in series **1** form a nematic phase with clearing temperatures in a range of 78–177 °C, while smectic phases were found only in **1[A]a**, **1[B]a**–**1[B]c** (Table 1, Fig. 3 and 4). Compounds **2[B]e** and **2[B]f** have the lowest T_{NI} in the series and are the only compounds with monotropic behavior. Surprisingly however, crystalline polymorphs obtained from melt have significantly lower melting points (63 °C [16] and 69 °C, respectively) and the nematic phase becomes enantiotropic for both compounds. Such a large difference in melting temperatures of crystalline polymorphs (ΔT = 58 K for **2[B]e**) is rarely observed for mesogens and never before for carborane derivatives.

TABLES 1 and 2

Comparative analysis demonstrates that *o*-carborane derivatives **1[B]** have lower clearing temperatures (T_c) and higher smectogenic character than the *p*-carborane analogues **1[A]**. For the first four members of the series, **1a**–**1d**, the difference in T_c is small (average ΔT_c = 7±2 K; Table 1, Fig. 5), while the difference for the pairs **2e** and **2f** is significantly greater (14 K and 23 K, respectively; Table 2). This decrease of phase stability upon substitution of *o*-carborane for *p*-carborane indicates the importance of increased lateral dipole–dipole interactions and arising from them relative difficulties in molecular packing in the mesophase particularly for **2[B]e** and **2[B]f** in which the bulky carborane unit is in the center of the rigid core. This corroborates with the observed significant increase of smectogenic behavior upon replacement of *p*-carborane with the isosteric *o*-carborane. Thus, a SmA phase is more stable by 76 K in **1[B]a**, than in the *p*-carborane analogue **1[A]a**, and in compounds **1b** and **1c** this stabilization is at least 45 K (Table 1). Moreover, a monotropic SmC phase was also detected in **1[B]a** (Fig. 4c).

Although *o*-carborane derivatives have relatively strong tendency to the formation of lamellar phases, this behavior is far from the smectogenic character of the benzene analogues **1[Ph]**. For instance, SmA phase is more stable by over 100 K in **1[Ph]a** than in **1[B]a**, and Schiff base **1[Ph]c** and stilbene

1[Ph]e exhibit rich smectic polymorphism (Tables 1 and 2). This observed difference in smectogenic behavior is related to the shape of the carborane and benzene and, consequently, to molecular packing of their derivatives in lamellar phases, as it was already postulated for *p*-carborane derivatives.[2] Interestingly, chiral azo ester **1[Ph]d** does not crystallize and exhibits an E phase at ambient temperature (Fig. 4d).

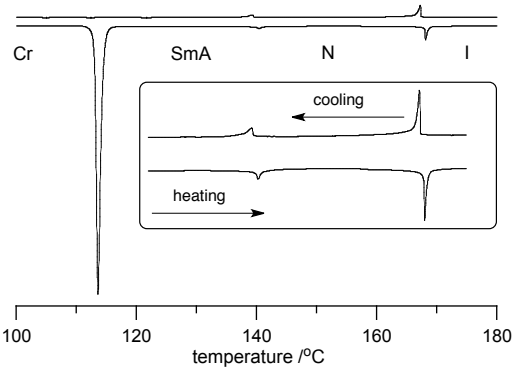

Fig. 3. DCS trace for **1[B]b**; heating rate 5 K min^{-1}. The inset shows a magnified portion of the trace with the SmA–N and N–I transitions.

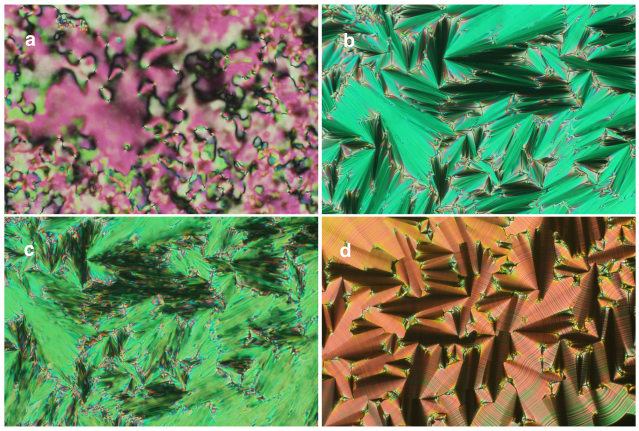

Fig. 4. Optical textures obtained by cooling from the isotropic phase of **1[B]a**: a) N (135 °C), b) SmA (100 °C) and c) SmC phase (30 °C), and of **1[Ph]d**: d) E phase (100 °C).

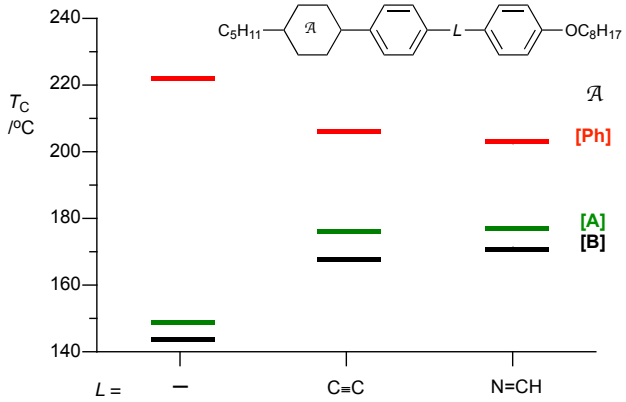

Fig. 5. Trends in mesophase stability (N–I or SmA–I transition temperatures) as a function of the linking group *L* in series **1**.

Series **1a**–**1c** permitted an analysis of the impact of the linking group *L* on mesophase stability. Thus, insertion of a two-atom fragment between the benzene rings in the terphenyl derivative **1[Ph]a** lowered the mesophase stability in **1[Ph]b** and **1[Ph]c** by nearly 20 K (Fig. 5) presumably due to increased flexibility of the core and lower packing fraction. In contrast, the analogous transformation of carborane derivatives **1[A]a** and **1[B]a** stabilized the nematic phase by about 25 K in the corresponding derivatives **1b** and **1c**. Also the SmA phase was significantly stabilized in the *o*-carborane derivatives **1[B]b** and **1[B]c** relative to **1[B]a**.

Molecular Modeling

For a better understanding of powder XRD results and the impact of substitution of *p*-carborane with *o*-carborane on molecular dimensions, molecular structures of selected compounds were fully optimized at the B3LYP/6-31G(2d,p) level of theory. Analysis of results demonstrated that the structurally analogous *o*-carborane and *p*-carborane derivatives are essentially isosteric with the total length of about 31 Å (for **1a**) or 33 Å (for **1b** and **1c**) in the most extended conformations (Fig. 6).[28] The benzene analogues are about 0.7 Å shorter than the corresponding carborane derivatives.

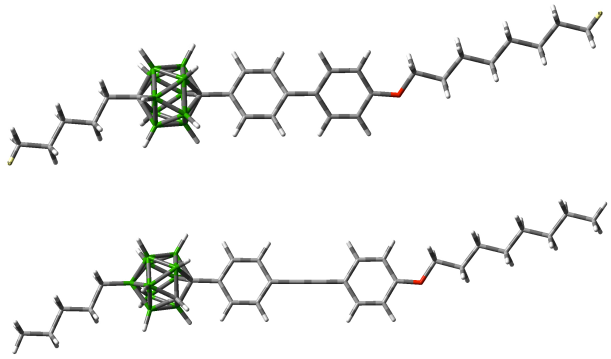

Fig. 6. Equilibrium geometry for **1[A]a** (upper) and **1[B]b** (lower) at the B3LYP/6-31G(2d,p) level of theory.

Powder XRD data

Analysis of smectic phases formed by *o*-carborane (**B**) derivatives revealed typical behavior: the layer thickness in SmA phase slightly increases with lowering temperature due to diminishing thermal motions (e.g. $\kappa = -9.65\pm0.08$ pm K^{-1} for **1[B]b**), while the SmC layer in **1[B]a** contracts rapidly due to the progression of the molecular tilt.[28] The observed interlayer spacing in the SmA phase is about 2 Å shorter than the calculated molecular lengths.

XRD analysis of benzene derivatives **1[Ph]a** – **1[Ph]c** confirmed their rich smectic polymorphism, as shown for **1[Ph]c** in Fig. 7. Thus, below SmA and SmC phases, there are more organized tilted smectic (SmI, SmF) and soft crystalline phases with transitions well marked by the changes of intensity of the diffraction signal related to the layer thickness. Phase identification was confirmed by analysis of the wide angle range of XRD patterns.[28] The transition from the SmC having liquid-like layers to a hexatic SmI is accompanied by a relatively large enthalpy of transition (3.6 kJ mol^{-1}), which is consistent with increasing positional correlations of molecules within the smectic layers. The measured layer spacing in the SmA phase is 32.3 Å, which correlated well with the calculated

molecular length of 32.4 Å. Similar analysis was performed for other benzene derivatives and details are listed in the ESI.

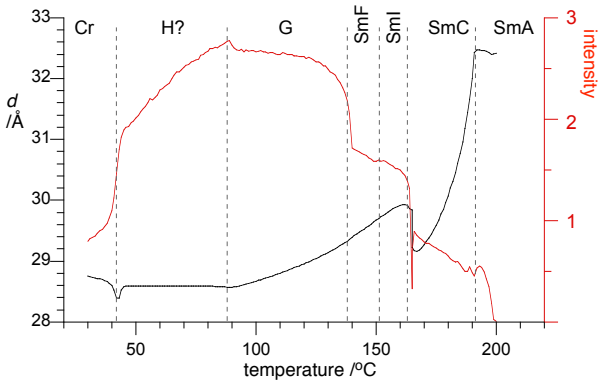

Fig. 7. Layer spacing *d* and intensity of related XRD signal for **1[Ph]c** as a function of temperature.

XRD analysis of **2[Ph]f** revealed a soft crystalline B phase instead of an E phase, which was previously reported[23] on the basis of microscopic observations.

Binary mixtures

To assess the impact of the molecular dipole moment of *o*-carborane on electrooptical properties, two isostructural biphenyls **1[A]a** and **1[B]a** were investigated as low concentration additives to **6CHBT**,[28-30] which is an ambient temperature nematic characterized by a positive Δε = +8.06.

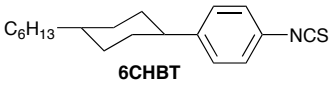

Thermal analysis of the binary mixtures demonstrated a linear dependence of the nematic-isotropic transition on concentration for the *p*-carborane derivative **1[A]a**, while the correlation for the *o*-carborane analogue **1[B]a** deviates from the linearity above 10 mol% (Fig. 8). Linear extrapolation of the mixture's N–I transition peak temperatures to the pure additive gave the virtual N–I transition temperatures [T_{NI}] of 187±3 °C for **1[A]a** and 148±3 °C for **1[B]a** in **6CHBT**. A comparison of the clearing temperatures for pure compounds (Table 1) with the extrapolated values [T_{NI}] demonstrates that the nematic phase of *p*-carborane **1[A]a** is stabilized by nearly 30 K in the host relative to the pure compound. Additional stabilization of the nematic phase is also apparent for **1[B]a** at higher concentrations (Fig. 8); however at concentrations <10 mol% the the mixture exhibits nearly ideal behavior.

Dielectric analysis of the binary mixtures in **6CHBT** at 1 kHz revealed linear dependence of dielectric parameters on concentration (Fig. 9), which, after extrapolation, established dielectric values shown in Table 3. As expected, the polar derivative **1[B]a** has a substantial longitudinal dielectric permittivity component $\varepsilon_{||}$ = 17.5 and, consequently, a significant positive dielectric anisotropy Δε = 11.0. In contrast, the *p*-carborane analogue **1[A]a** has a small negative Δε = –1.1, resulting from unrealistically low $\varepsilon_{||}$ = 0.2.

The carborane additives also affect elastic constants of the host: both compounds systematically increase splay and twist constants K_{11} and K_{22}, although the effect is smaller for the *o*-carborane derivative **1[B]a**. For instance both values are higher by about 30% for 10 mol% solutions. Further analysis indicates that the *p*-carborane derivative **1[A]a** lowers the rotational viscosity of the host, while the results for the **1[B]a** analogue are ambiguous.

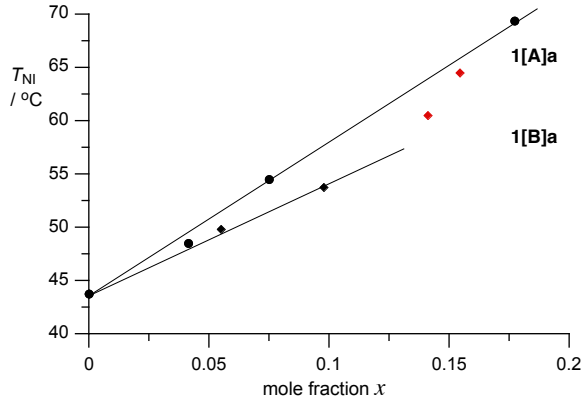

Fig. 8. A plot of peak temperature of the N–I transition for binary mixtures of **1[A]a** (circles) and **1[B]a** (diamonds) in **6CHBT**.

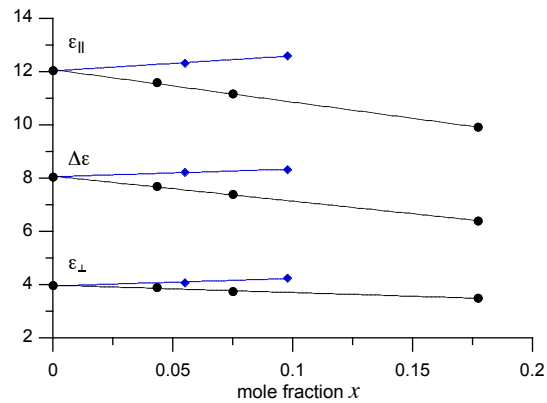

Fig. 9. Dielectric parameters of binary mixtures of **1[A]a** (black) and **1[B]a** (blue) in **6CHBT** as a function of concentration.

Table 3. Extrapolated experimental (upper) and predicted (lower) dielectric data and results of Maier-Meier analysis for **1[A]a** and **1[B]a**. [a]

Compd		$\varepsilon_{\parallel}$	$\varepsilon_{\perp}$	Δε	S_{app}	g
1[A]a	exp	0.2	1.3	-1.1	0.45	-2.06
	theory	5.0 [b]	3.5 [b]	1.5 [b]	0.67 [c]	0.45 [c]
1[B]a	exp	17.5	6.5	11.0	0.60	0.28
	theory	26.9 [b]	7.9 [b]	19.0 [b]	0.67 [c]	0.45 [c]

[a] For details see text and the ESI. Typical error of extrapolated dielectric parameters is ±0.20. [b] Calculated value assuming host's order parameter S = 0.67 and g = 0.45. [c] Assumed values.

Analysis of dielectric data

Dielectric parameters extrapolated for pure additives were analyzed using the Maier-Meier relationship (eq 1),[31,32] which connects molecular and phase parameters. Using experimental $\varepsilon_{\parallel}$ and Δε values (Table 3) and DFT-calculated parameters μ, α, and β (Table 4), equations 2 and 3 permitted the calculation of the apparent order parameter S_{app} and the Kirkwood factor $g = \mu^2_{eff}/\mu^2$ shown in Table 3. The effect of the additive was neglected and the field parameters F and h in equations 2 and 3 were calculated using the experimental dielectric and optical data for pure **6CHBT** host.[28-30]

$$\Delta\varepsilon = \frac{NFh}{\varepsilon_0}\left\{\Delta\alpha - \frac{F\mu_{eff}^2}{2k_BT}(1-3cos^2\beta)\right\} \quad \text{eq 1}$$

$$S_{app} = \frac{2\Delta\varepsilon\varepsilon_0}{NFh[2\Delta\alpha+3\bar{\alpha}(1-3cos^2\beta)]-3(\bar{\varepsilon}-1)\varepsilon_0(1-3cos^2\beta)} \quad \text{eq 2}$$

$$g = \frac{[(\varepsilon_{\parallel}-1)\varepsilon_0-\bar{\alpha}NFh-\frac{2}{3}\Delta\alpha NFhS_{app}]3k_BT}{NF^2h\mu^2[1-(1-3cos^2\beta)S_{app}]} \quad \text{eq 3}$$

Molecular electric dipole moment μ and polarizability α required for the Maier-Meier analysis of dielectric results were obtained at the B3LYP/6-31+G(2d,p)//B3LYP/6-31G(2d,p) level of theory in the dielectric medium of the host.[28]

Table 4. Calculated molecular parameters for **1[A]a** and **1[B]a**. [a]

Compd	$\mu_{\parallel}$ /D	$\mu_{\perp}$ /D	μ /D	β [b] /°	Δα /Å^3	α_{avrg} /Å^3
1[A]a	1.63	1.12	1.98	34.5	48.2	84.6
1[B]a	8.24	2.93	8.75	19.6	49.9	85.3

[a] Obtained at the B3LYP/6-31+G(2d,p)// B3LYP/6-31G(2d,p) level of theory in **6-CHBT** dielectric medium. For details see text and the ESI. [b] Angle between the net dipole vector μ and $\mu_{\parallel}$.

Data in Table 4 demonstrate that the replacement of *p*-carborane with *o*-carborane increases particularly strongly the longitudinal dipole moment component. The modest dipole moment of *p*-carborane derivative **1[A]a**, μ = 1.98 D, results from a combination of mainly two local dipole moments associated with the weakly polar alkoxyphenyl group and polarization from the electron-donating alkoxy group to the electron withdrawing carborane unit (σ_p = 0.12).[33] The resulting net dipole is oriented at 34.5° relative to the molecular axis of inertia. Substitution of the *o*-carborane for *p*-carborane in **1[A]a** increases polarization of the rigid core in **1[B]a** due to a higher electron-withdrawing character of the cluster (σ_p = 0.43)[34] and also introduces a reinforcing additional local dipole associated with the cage itself (Fig. 10). This results in a substantial longitudinal dipole moment component, $\mu_{\parallel}$ = 8.24 D, and a smaller angle β ≈ 20° (Table 4). Thus, on the basis of the calculated molecular dipole moment it is expected that the *p*-carborane derivative **1[A]a** will exhibit a small positive value of dielectric anisotropy, Δε = 1.5, while the *o*-carborane **1[B]a** will possess a significant Δε = 19.0, assuming host's order parameter *S* = 0.67 and a reasonable Kirkwood factor *g* = 0.45 (Table 3). Experimental dielectric values are, however, significantly smaller.

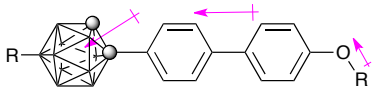

Fig. 10. Major local dipole moments in **1[B]a**.

Experimental data in Table 3 show that the dielectric parameters for **1[B]a** are smaller than expected, especially the $\varepsilon_{\parallel}$ component (17.5 instead of 26.9). Consequently, the calculated apparent order parameter S_{app} is lower than that for the host, and the Kirkwood factor *g* is unusually small (0.28) at concentrations <10 mol%; the latter parameter may indicate significant aggregation in the solution, while the S_{app} suggests poor alignment of the molecules (presumably aggregates) in the nematic phase. The dielectric results for the *p*-carborane analogue **1[A]a** are more difficult to rationalize: while the low value of S_{app} is small but acceptable, the negative *g* factor is physically unrealistic, although consistent with the unrealistically low extrapolated $\varepsilon_{\parallel}$ = 0.2 (predicted 5.0, Table 3). Similar results were obtained for solutions of another *p*-carborane derivative in **6CHBT**,[19] which presumably reflect molecular dynamics at 1 kHz and specific solute-solvent interactions. In all cases, the unusually low extrapolated $\varepsilon_{\parallel}$ results in excessively negative extrapolated Δε values.

Discussion

The recent availability[16] of isomerically pure derivatives **8** and **9** opened the way to a new class of polar mesogens based on *o*-carborane (Fig. 11). In general, these currently available precursors permit incorporation of motifs **I** and **II** into the molecular structure as either a terminal or central part of the rigid core. Thus far, the B(12)–I group was used for B-alkylation (Negishi pentylation of **8**) and B-arylation (pentyloxyphenylation of **9**) reactions, and the vinyl group in **9** was arylated in the Heck coupling,[16] however other C–C coupling reactions and synthesis of other intermediates are possible to expand the structural variety and fine-tuning of molecular and bulk properties of the materials. The first series of *o*-carborane-containing mesogens presented here was obtained using mainly 4-halophenyl derivatives **3[B]** and aniline **4[B]**, which can serve as versatile precursors to other similar mesogenic derivatives.

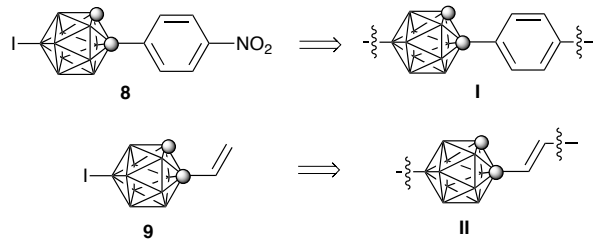

Fig. 11. Precursors **8** and **9** derived from them molecular fragments **I** and **II**.

Results for the handful of available mesogenic *o*-carborane derivatives demonstrate that compounds containing fragment **I** (series **1[B]**) exhibit greater propensity to the formation of smectic phases than those in series **2[B]**. This is presumably because of the position of the bulky carborane unit in the molecule: in **1[B]** it resides at the edge of the rigid core, which is more favorable for the formation of lamellar phases further enhanced by lateral dipole-dipole interactions.

A comparison of mesogenic derivatives of *o*-carborane with the isosteric *p*-carborane analogues provides an excellent opportunity for a better understanding of the fundamental issue of the role of a molecular dipole moment in phase stability. In recent years, we have demonstrated that replacement of the non-polar C–C bond in carborane derivatives with the isosteric polar B–N bond introduces a substantial longitudinal dipole moment of 12 D in 10-vertex and 10 D in 12-vertex derivatives.[14,15] This replacement generally increases the nematic phase stability by up to 55 K, and, surprisingly, does not induce smectic polymorphism. In the present work, we compare isomeric carborane derivatives, which result from the exchange of positions of cluster's B and C atoms. The results

show that phases formed by the polar *o*-carborane derivatives are less thermodynamically stable and smectic polymorphism is more pronounced, when compared to the weakly polar *p*-carborane analogues. The compounds are essentially isosteric but conformational properties of the carborane–aryl(alkyl) bond differ somewhat due to the relatively short C–C bond in *o*-carborane. This is evident from the analysis of molecular models for **1[B]** and consistent with experimental data for 1-phenyl-*o*-carborane[35] (Fig. 12).

Fig. 12. A pseudo-Newman projection of a conformational minimum of 1-phenyl-*o*-carborane (ref[35]). The bar represents the benzene ring plane and the spheres are the carbon atoms.

Dielectric data for the two carborane derivatives **1[A]a** and **1[B]a** show smaller than expected $\varepsilon_{\parallel}$ components (hence lower $\Delta\varepsilon$ values), presumably due to specific polar solvent – polar solute interactions,[36] molecular aggregation,[37] and/or molecular dynamics; the former depend on the host, while the dynamics on the frequency used in the measurement. If the low $\varepsilon_{\parallel}$ value is due mainly to the frequency of the oscillating electric field (which is plausible especially for the weakly polar **1[A]a**), then both compounds may exhibit a low cross-over frequency f_c (where $\Delta\varepsilon$ changes the sign) just above the measuring frequency (1 kHz). In such a case, compounds of this type, in which there is a large heavy substituent (the carborane cage) at the end of the rigid core with a significant moment of inertia, are potentially suitable for formulation of materials for dual-frequency addressing of LC displays.[38,39] This warrants further detailed investigation of such derivatives with dielectric spectroscopy tools.

Summary and Conclusions

A strategy to a potentially broad series of liquid crystalline derivatives of the polar *o*-carborane has been developed and demonstrated on a handful of derivatives. These derivatives exhibit somewhat lower clearing temperatures and higher smectic phase stability than the analogous derivatives of *p*-carborane. The inherent dipole moment of *o*-carborane cage gives rise to a substantial molecular dipole moment oriented along the main axis, which results in sizable dielectric anisotropy ($\Delta\varepsilon$ = 11.0 in **6CHBT** host at 1 kHz) and makes such derivatives attractive for electrooptical applications. Also the combination of smectogenic character and inherent polarity of *o*-carborane derivatives is of interest for the development of materials for FLC and AFLC applications. Initial results also suggest that derivatives of type **1** may have a relatively low cross-over frequency f_c and thus may be attractive for dual-frequency devices. These results warrant further exploration of mesogenic carborane derivatives as additives to nematic and smectic hosts.

Computational Details

Quantum-mechanical calculations were carried out using Gaussian 09 suite of programs.[40] Geometry optimizations for unconstrained conformers of **1a** with most extended molecular shapes were undertaken at the B3LYP/6-31G(2d,p) level of theory using default convergence limits. Vibrational frequencies were used to characterize the nature of the stationary points and to obtain exact polarizabilities in vacuum. The alkyl groups were in all-*trans* conformation. No conformational search was attempted. Final coordinates for each molecular model are provided in the ESI.

Dipole moments and exact electronic polarizabilities of **1a** used in the Maier–Meier data analysis were obtained in **6CHBT** dielectric medium using the B3LYP/6-31+G(2d,p)// B3LYP/6-31G(2d,p) method and the PCM solvation model[41] requested with SCRF(Solvent=Generic, Read) keywords and "eps=6.70" and "epsinf=2.4623" parameters (single point calculations). Exact polarizabilities were obtained using the POLAR keyword. The reported values for dipole moment components and dielectric permittivity tensors are at Gaussian standard orientation of each molecule (charge based), which is close to the principal moment of inertia coordinates (mass based), are listed in the ESI.

Experimental Section

General. NMR spectra were obtained at 400.1 MHz (^{1}H), 125 MHz (^{13}C), and 128.4 MHz (^{11}B), using a 9.4 T Bruker or JOEL ECX 500 instrument in $CDCl_3$, unless specified otherwise. ^{1}H NMR spectra were referenced to the solvent and ^{11}B NMR chemical shifts to an external boric acid sample in CH_3OH that was set to 18.1 ppm. Thermal analysis was obtained using a TA Instruments DSC 2920 using small samples of about 0.5-1.0 mg. IR spectra were recorded in KBr pellets using ATI Mattson Infinity FTIR 60. HRMS data were obtained on a Bruker micrOTOF II instrument. MALDI-TOF mass data were acquired using a Voyager Elite instrument.

Binary mixtures preparation. Solutions of carborane derivatives **1a** in **6CHBT** host (15-20 mg of the host) were prepared in an open vial. A mixture of the compound and the host in CH_2Cl_2 was heated for 2 hr at 60 ^{o}C to remove the solvent and evacuated (10^{-2} Torr). The resulting binary mixtures were analyzed by polarized optical microscopy (POM, PZO Biolar) to ensure homogeneity. The mixtures were then allowed to stand for 2 hr at room temperature before thermal and dielectric measurements.

Electrooptical measurements. Dielectric properties of solutions of selected compound in **6CHBT** were measured by a Liquid Crystal Analytical System (LCAS - Series II, LC Vision, Inc.) using GLCAS software version 0.13.14, which implements literature procedures for dielectric constants. The instrument was calibrated using a series of capacitors. The homogenous binary mixtures were loaded into ITO electro-optical cells by capillary forces with moderate heating supplied by a heat gun. The cells (about 10 μm thick, electrode area 1.00 cm^2 and anti-parallel rubbed polyimide layer) were obtained from LC Vision, Inc. The filled cells were heated to an isotropic phase and cooled to rt before measuring the dielectric

properties. Default parameters were used for measurements: triangular shaped voltage bias ranging from 0.1-20 V at 1 kHz frequency. The threshold voltage V_{th} was measured at a 5% change. For each mixture the measurement was repeated 10 times manually for two cells. The results were averaged to calculate the mixture's parameters. Results are provided in ESI and extrapolated values for pure additives are shown in Table 3.

Preparation of derivatives of tolanes 1b. General procedure. To a solution of 4-octyloxyphenylacetylene[21,22] (0.35 mmol), iodoarene **3** (0.30 mmol) in dry THF (3 mL) and Hunig's base (0.2 mL) were added at rt under Ar atmosphere, followed by $Pd(PPh_3)_2Cl_2$ (0.03 mmol) and CuI (0.015 mmol). The mixture was stirred at rt for 2-3 h, 5% HCl was added, organic products were extracted (CH_2Cl_2), extracts dried (Na_2SO_4), and solvents were evaporated. The crude product was purified on a silica gel plug (CH_2Cl_2/hexane, 1:5) followed by repeated recrystallization (hexane and EtOH/EtOAc).

4-(12-C_5H_{11}-*p*-carboran-1-yl)$C_6H_4C{\equiv}CC_6H_4OC_8H_{17}$ (1[A]b). White solid: ^{1}H NMR (400 MHz, $CDCl_3$) δ 0.84 (t, *J* = 7.3 Hz, 3H), 0.88 (t, *J* = 6.8 Hz, 3H), 1.08-1.38 (m, 8H), 1.45 (quint, *J* = 7.4 Hz, 2H), 1.50-4.0 (m, 10H), 1.65 (br t, *J* = 8.4 Hz, 2H), 1.78 (quint, *J* = 7.1 Hz, 2H), 3.96 (t, *J* = 6.6 Hz, 2H), 6.84 (d, *J* = 8.8 Hz, 2H), 7.15 (d, *J* = 8.6 Hz, 2H), 7.27 (d, *J* = 8.6 Hz, 2H), 7.40 (d, *J* = 8.8 Hz, 2H); ^{13}C NMR (125 MHz, $CDCl_3$) δ 13.9, 14.1, 22.2, 22.6, 26.0, 29.16, 29.22, 29.33, 29.7, 31.2, 31.8, 37.9, 68.1, 80.5 (br), 81.6 (br), 87.0, 90.7, 114.5, 114.8, 123.7, 127.2, 130.9, 133.0, 135.9, 160.0; ^{11}B NMR (128 MHz, $CDCl_3$) δ -12.3 (d, *J* = 164 Hz); IR (KBr) ν 2607 (B–H), 2217 (C≡C), 1516, 1247 cm^{-1}; MALDI-TOF (ANP) *m/z* 516.5–521.5 (max at 519.5, $[M]^+$). Anal. Calcd for $C_{29}H_{46}B_{10}O$: C, 67.14; H, 8.94. Found: C, 67.15; H, 9.05.

4-(12-C_5H_{11}-*o*-carboran-1-yl)$C_6H_4C{\equiv}CC_6H_4OC_8H_{17}$ (1[B]b). White solid: ^{1}H NMR (400 MHz, $CDCl_3$) δ 0.73 (br t, *J* = 6.6 Hz, 2H), 0.87 (t, *J* = 6.6 Hz, 3H), 0.89 (t, *J* = 7.4 Hz, 3H), 1.20-1.39 (m, 14H), 1.50-4.0 (m, 9H), 1.45 (quint, *J* = 7.3 Hz, 2H), 1.77 (quint, *J* = 7.1 Hz, 2H), 3.90 (br s, 1H), 3.97 (t, *J* = 6.6 Hz, 2H), 6.86 (d, *J* = 8.8 Hz, 2H), 7.41-7.48 (m, 6H); MALDI-TOF (CHCA) *m/z* 516.5–521.5 (max at 519.5, $[MH]^+$). Anal. Calcd for $C_{29}H_{46}B_{10}O$: C, 67.14; H, 8.94. Found: C, 67.07; H, 8.93.

4-(12-C_5H_{11}-C_6H_4)$C_6H_4C{\equiv}CC_6H_4OC_8H_{17}$ (1[Ph]b). White solid: ^{1}H NMR (400 MHz, CD_2Cl_2) δ 0.90 (t, *J* = 7.0 Hz, 3H), 0.91 (t, *J* = 6.8 Hz, 3H), 1.23-1.40 (m, 12H), 1.46 (quint, *J* = 7.6 Hz, 2H), 1.65 (quint, *J* = 7.6 Hz, 2H), 1.79 (quint, *J* = 7.5 Hz, 2H), 2.65 (t, *J* = 7.7 Hz, 2H), 3.98 (t, *J* = 6.6 Hz, 2H), 6.88 (d, *J* = 8.8 Hz, 2H), 7.27 (d, *J* = 8.2 Hz, 2H), 7.46 (d, *J* = 8.8 Hz, 2H), 7.53 (d, *J* = 8.1 Hz, 2H), 7.56 and 7.59 (AB, *J* = 8.5 Hz, 4H); ^{13}C NMR (125 MHz, $CDCl_3$) δ 14.0, 14.1, 22.5, 22.7, 26.0, 29.19, 29.22, 29.3, 31.2, 31.5, 31.8, 35.6, 68.1, 88.0, 90.0, 114.5, 115.1, 122.2, 126.75, 126.79, 128.9, 131.8, 133.0, 137.7, 140.5, 142.5, 159.2; IR (KBr) ν 2212 (C≡C), 1604, 1510, 1246 cm^{-1}; MALDI-TOF (ANP) *m/z* 452.3 ($[M]^+$) and 453.3 ($[M+1]^+$]. Anal. Calcd for $C_{33}H_{40}O$: C, 87.56; H, 8.91. Found: C, 87.26; H, 8.88.

Preparation of azomethine derivatives 1c. General procedure. A mixture of appropriate aniline **4** (0.15 mmol), 4-octyloxybenzaldehyde[42] (0.15 mmol) and cat. amounts of AcOH in EtOH (2 mL) was refluxed for 1 h. Solvent was evaporated and the crude product was recrystallized repeatedly from hexane.

4-(12-C_5H_{11}-*p*-carboran-1-yl)$C_6H_4N{=}CHC_6H_4OC_8H_{17}$ (1[A]c). White solid, (80% yield): ^{1}H NMR (400 MHz, $CDCl_3$) δ 0.84 (t, *J* = 7.3 Hz, 3H), 0.89 (t, *J* = 6.9 Hz, 3H), 1.05-1.40 (m, 14H), 1.50-4.0 (m, 10H), 1.46 (quint, *J* = 7.4 Hz, 2H), 1.65 (br t, *J* = 8.4 Hz, 2H), 1.80 (quint, *J* = 7.1 Hz, 2H), 4.01 (d, *J* = 6.6 Hz, 2H), 6.94 (d, *J* = 8.9 Hz, 2H), 6.95 (d, *J* = 8.8 Hz, 2H), 7.19 (d, *J* = 8.7 Hz, 2H), 7.78 (d, *J* = 8.7 Hz, 2H), 8.27 (s, 1H); ^{11}B NMR (128 MHz, $CDCl_3$) δ -12.3 (d, *J* = 164 Hz); IR (KBr) ν 2606 (B–H), 1696 (N=C), 1601, 1509, 1256 cm^{-1}; MALDI-TOF (CHCA) *m/z* 520.6–524.6 (max at 523.6, $[MH]^+$). Anal. Calcd for $C_{28}H_{47}B_{10}NO$: C, 64.45; H, 9.08; N, 2.68. Found: C, 64.64; H, 9.19; N, 2.71.

4-(12-C_5H_{11}-*o*-carboran-1-yl)$C_6H_4N{=}CHC_6H_4OC_8H_{17}$ (1[B]c). White solid, (78% yield): ^{1}H NMR (400 MHz, $CDCl_3$) δ 0.73 (t, *J* = 7.3 Hz, 2H), 0.87 (t, *J* = 7.0 Hz, 3H), 0.89 (t, *J* = 6.7 Hz, 3H), 1.22-1.41 (m, 14H), 1.50-4.0 (m, 9H), 1.47 (quint, *J* = 7.1 Hz, 2H), 1.81 (quint, *J* = 7.1 Hz, 2H), 3.90 (br s, 1H), 4.02 (d, *J* = 6.6 Hz, 2H), 6.97 (d, *J* = 8.8 Hz, 2H), 7.09 (d, *J* = 8.7 Hz, 2H), 7.50 (d, *J* = 8.7 Hz, 2H), 7.81 (d, *J* = 8.8 Hz, 2H), 8.31 (s, 1H). Anal. Calcd for $C_{28}H_{47}B_{10}NO$: C, 64.45; H, 9.08; N, 2.68. Found: C, 64.39; H, 9.11; N, 2.65.

4-(4-$C_5H_{11}C_6H_4$)$C_6H_4N{=}CHC_6H_4OC_8H_{17}$ (1[Ph]c). Off-white solid, (80% yield): ^{1}H NMR (400 MHz, $CDCl_3$) δ 0.90 (t, *J* = 7.0 Hz, 3H), 0.91 (t, *J* = 6.8 Hz, 3H), 1.24-1.41 (m, 12H), 1.48 (t, *J* = 7.4 Hz, 2H), 1.66 (quint, *J* = 7.6 Hz, 2H), 1.82 (quint, *J* = 7.1 Hz, 2H), 2.65 (t, *J* = 7.8 Hz, 2H), 4.03 (t, *J* = 6.6 Hz, 2H), 6.98 (d, *J* = 8.8 Hz, 2H), 7.24-7.28 (m, 4H), 7.53 (d, *J* = 8.2 Hz, 2H), 7.61 (d, *J* = 8.5 Hz, 2H), 7.85 (d, *J* = 8.7 Hz, 2H), 8.44 (s, 1H); ^{13}C NMR (125 MHz, $CDCl_3$) δ 14.0, 14.1, 22.6, 22.7, 26.0, 29.16, 29.23, 29.34 31.2, 31.5, 31.8, 35.6, 68.2, 114.7, 121.3, 126.7, 127.6, 128.8, 130.7 (br), 138.0, 138.5, 142.0, 159.4, 162.0; IR (KBr) ν 1606, 1252 cm^{-1}; MALDI-TOF (CHCA) *m/z* 456.4 ($[MH]^+$) and 457.4 ($MH+1]^+$). Anal. Calcd for $C_{32}H_{41}NO$: C, 84.35; H, 9.07; N, 3.07. Found: C, 84.14; H, 9.18; N, 3.11.

Preparation of azobenzene derivatives 1d. General procedure. A mixture of appropriate aniline **4** (0.15 mmol), (*S*)-2-methylbutyl 4-nitrosobenzoate (**5**, 0.15 mmol) and catalytic amounts of AcOH in CH_2Cl_2 (1 mL) was stirred at rt under Ar for 24 h. Reaction with aniline **4[B]** (*o*-carborane) was conducted in AcOH (1 mL). Solvents and AcOH were removed under reduced pressure and the orange crude product was purified on a silica gel plug (hexane/CH_2Cl_2, 3:1) and then recrystallized repeatedly from EtOH.

4-(12-C_5H_{11}-*p*-carboran-1-yl)$C_6H_4N{=}NC_6H_4COOC_5H_{11}$* (1[A]d). Orange solid: ^{1}H NMR (400 MHz, $CDCl_3$) δ 0.85 (t, *J* = 7.2 Hz, 3H), 0.95 (t, *J* = 7.4 Hz, 3H), 1.03 (d, *J* = 6.7 Hz, 3H), 1.06-1.34 (m, 6H), 1.50-3.50 (m, 10H), 1.66 (br t, *J* = 8.5

Hz, 2H), 1.89 (sext, J = 7.1 Hz, 1H), 4.16 (dd, J_1 = 10.7 Hz, J_2 = 6.6 Hz, 1H), 4.24 (dd, J_1 = 10.7 Hz, J_2 = 6.0 Hz, 1H), 7.37 (d, J = 8.8 Hz, 2H), 7.73 (d, J = 8.8 Hz, 2H), 7.90 (d, J = 8.6 Hz, 2H), 8.17 (d, J = 8.6 Hz, 2H); ^{11}B NMR (128 MHz, $CDCl_3$) δ -12.3 (d, J = 164 Hz); IR (KBr) ν 2609 (B–H), 1716 (C=O), 1272 (C–O) cm^{-1}; MALDI-TOF (CHCA) m/z 506.5–512.5 (max at 510.5, $[MH]^+$). Anal. Calcd for $C_{25}H_{40}B_{10}N_2O_2$: C, 59.03; H, 7.93; N, 5.51. Found: C, 59.09; H, 7.85; N, 5.44.

4-(12-C_5H_{11}-*o*-carboran-1-yl)C_6H_4N=NC_6H_4COOC_5H_{11}* (1[B]d). Orange solid: ^{1}H NMR (400 MHz, $CDCl_3$) δ 0.75 (br t, J = 7.8 Hz, 2H), 0.88 (t, J = 6.6 Hz, 3H), 0.98 (t, J = 7.4 Hz, 3H), 1.04 (d, J = 6.8 Hz, 3H), 1.22-1.36 (m, 14H), 1.50-4.0 (m, 9H), 1.50-1.62 (m, 2H), 1.81 (sext, J = 7.1 Hz, 1H), 3.98 (br s, 1H), 4.17 (dd, J_1 = 10.7 Hz, J_2 = 6.6 Hz, 1H), 4.25 (dd, J_1 = 10.7 Hz, J_2 = 6.0 Hz, 1H), 7.66 (d, J = 8.8 Hz, 2H), 7.88 (d, J = 8.8 Hz, 2H), 7.95 (d, J = 8.6 Hz, 2H), 8.20 (d, J = 8.6 Hz, 2H); ^{13}C NMR (125 MHz, $CDCl_3$) δ 11.2, 14.0, 16.5, 22.6, 26.3, 29.5, 29.7, 34.3, 35.1, 58.9, 69.3, 67.0, 122.9, 123.2, 128.8, 130.6, 132.8, 136.1, 152.8, 154.8, 166.0; ^{11}B NMR (160 MHz, $CDCl_3$) δ -10.7 (m, 5B), -7.5 (d, J = 146 Hz, 2B), -0.7 (d, J = 148 Hz, 2B), 8.5 (br s, 1B); MALDI-TOF (CHCA) m/z 507.5–512.5 (max at 510.5, $[MH]^+$). Anal. Calcd for $C_{25}H_{40}B_{10}N_2O_2$: C, 59.03; H, 7.93; N, 5.51. Found: C, 59.39; H, 7.99; N, 5.50.

4-(4-$C_5H_{11}C_6H_4$)C_6H_4N=NC_6H_4COOC_5H_{11}* (1[Ph]d). Orange solid: ^{1}H NMR (400 MHz, $CDCl_3$) δ 0.92 (t, J = 6.7 Hz, 3H), 0.98 (t, J = 7.5 Hz, 3H), 1.05 (d, J = 6.7 Hz, 3H), 1.20-1.43 (m, 6H), 1.50-1.62 (m, 2H), 1.67 (quint, J = 7.5 Hz, 2H), 1.89 (sext, J = 7.1 Hz, 1H), 2.67 (t, J = 7.7 Hz, 2H), 4.17 (dd, J_1 = 10.7 Hz, J_2 = 6.6 Hz, 1H), 4.25 (dd, J_1 = 10.7 Hz, J_2 = 6.0 Hz, 1H), 7.30 (d, J = 8.1 Hz, 2H), 7.60 (d, J = 8.1 Hz, 2H), 7.76 (d, J = 8.5 Hz, 2H), 7.97 (d, J = 8.4 Hz, 2H), 8.02 (d, J = 8.4 Hz, 2H), 8.20 (d, J = 8.5 Hz, 2H). Anal. Calcd for $C_{29}H_{34}N_2O_2$: C, 78.70; H, 7.74; N, 6.33. Found: C, 78.12; H, 7.69; N, 6.20.

4-(12-(4-$C_5H_{11}OC_6H_4$)-*o*-carboran-1-yl)$CH_2CH_2C_6H_4OC_5H_{11}$ (2[B]f). Styrene derivative[16] **2[B]e** was reduced with H_2 (50 psi) in the presence of Pd/C (10%) in THF. The reaction mixture was filtered, solvent was evaporated and the resulting crude product was passed through a silica gel plug (CH_2Cl_2/hexanes, 1:2) followed by recrystallization (pentane, –78 °C followed by MeOH, –5 °C) giving the desired product as a white solid: ^{1}H NMR (500 MHz, $CDCl_3$) δ 0.91 (t, J = 6.9 Hz, 3H), 0.93 (t, J = 6.9 Hz, 3H), 1.33-1.47 (m, 8H), 1.72-1.80 (m, 4H), 2.50 and 2.73 (A_2X_2, 4H), 3.64 (br s, 1H), 3.91 (t, J = 6.9 Hz, 2H), 3.92 (t, J = 6.9 Hz, 2H), 6.76 (d, J = 8.6 Hz, 2H), 6.82 (d, J = 8.6 Hz, 2H), 7.03 (d, J = 8.6 Hz, 2H), 7.27 (d, J = 8.6 Hz, 2H); ^{13}C NMR (125 MHz, $CDCl_3$) δ 14.0 (2C), 22.5 (2C), 28.20, 28.22, 28.96, 29.02, 34.6, 39.2, 59.9, 67.7, 68.1, 68.6 (br), 113.6, 114.8, 129.1, 130.5, 133.6, 158.0, 158.8; ^{11}B NMR (160 MHz, $CDCl_3$) δ –11.4 (m, 4B), –7.9 (d, J = 158 Hz, 3B), –1.2 (d, J = 151 Hz, 2B), +5.8 (br s, 1B). ESI–HRMS, calcd for $C_{26}H_{44}B_{10}O_2$•Na $[M\text{-}Na]^+$ m/z 521.4169; found m/z 521.4185.

1-(4-Iodophenyl)-12-pentyl-*p*-carborane (3[A], Hal=I). To a solution of bromophenyl derivative[17] **3[A]** (Hal=Br, 100 mg, 0.27 mmol) in THF (10 mL), n-BuLi in hexanes (0.33 mmol) was added at –78 °C. After 1 hr solid I_2 was added and the mixture was stirred for 1 hr. The solvent was evaporated, and the residue was passed through a silica gel plug (hexanes). The crude product (90 mg, containing some dehalogenated derivative) was purified by recrystallization (hexane, –10 °C) giving the iodide **3[A], Hal=I** as a white solid: ^{1}H NMR (400 MHz, $CDCl_3$) δ 0.84 (t, J = 7.3 Hz, 3H), 1.05-1.27 (m, 6H), 1.50-3.50 (m, 10H), 1.64 (br t, J = 8.3 Hz, 2H), 6.93 (d, J = 8.7 Hz, 2H), 7.49 (d, J = 8.7 Hz, 2H); ^{11}B NMR (128 MHz, $CDCl_3$) δ -12.4 (d, J = 165 Hz). ESI–HRMS calcd for $C_8H_{14}B_{10}I$ $[M–C_5H_{11}]^+$ m/z 347.1078; found m/z 347.1053.

1-(4-Aminophenyl)-12-pentyl-*p*-carborane (4[A]). The nitrophenyl derivative **6[A]** (250 mg, 0.75 mmol) in THF (10 mL) was hydrogenated (40 psi) in the presence of 10% Pd/C (25 mg) for 2 hrs. The catalyst was filtered off, the solvent was evaporated, and the resulting crude product was purified by SiO_2 plug (CH_2Cl_2) giving 180 mg (79% yield) of amine **4[A]** as a white solid: mp 85.4-86.0 °C; ^{1}H NMR (400 MHz, $CDCl_3$) δ 0.83 (t, J = 7.3 Hz, 3H), 1.05-1.27 (m, 6H), 1.50-3.50 (m, 10H), 1.63 (br t, J = 8.4 Hz, 2H), 4.00 (br s, 2H), 6.46 (d, J = 8.7 Hz, 2H), 6.97 (d, J = 8.7 Hz, 2H); ^{13}C NMR (125 MHz, $CDCl_3$) δ 13.9, 22.2, 29.2, 31.2, 37.8, 80.4 (br), 81.2 (br), 114.6, 127.2, 128.2, 145.5; ^{11}B NMR (128 MHz, $CDCl_3$) δ -12.4 (d, J = 165 Hz); MALDI-TOF (CHCA) m/z 303.4–307.4 (max at 306.4, $[M]^+$). Anal. Calcd for $C_{13}H_{27}B_{10}N$: C, 51.11; H, 8.91; N, 4.59. Found: C, 51.58; H, 9.03; N, 4.63.

(*S*)-2-Methylbutyl 4-nitrosobenzoate (5). Following the general procedure,[27] to a solution of (*S*)-2-methylbutyl 4-aminobenzoate[25,26] (**7**, 310 mg, 1.5 mmol) in CH_2Cl_2 (5 mL), a solution of Oxone® (1.85 g, 3.0 mmol) in water (18 mL) was added under Ar. The mixture was stirred overnight at rt, the organic layer was separated, dried (Na_2SO_4), and solvent was evaporated. The crude product was separated from unreacted starting materials on a short silica gel plug (hexane/CH_2Cl_2, 5:1) to give 100 mg (30% yield) of the nitroso ester **5** as a yellow-green viscous oil, which was used immediately for the next transformation. ^{1}H NMR (400 MHz, $CDCl_3$) δ 0.98 (t, J = 7.5 Hz, 3H), 1.04 (d, J = 6.8 Hz, 3H), 1.25-1.34 (m, 1H), 1.49-1.60 (m, 1H), 1.89 (sext, J = 6.6 Hz, 1H), 4.19 (dd, J_1 = 10.8 Hz, J_2 = 6.6 Hz, 1H), 4.27 (dd, J_1 = 10.8 Hz, J_2 = 6.0 Hz, 1H), 7.94 (d, J = 8.6 Hz, 2H), 8.30 (d, J = 8.6 Hz, 2H).

1-(4-Nitrophenyl)-12-pentyl-*p*-carborane (6[A]). To a solution of *p*-carborane (0.500 g, 3.50 mmol) in dry THF (10 mL), under Ar at –78 °C, n-BuLi was added (3.8 mmol). After 0.5 h, the mixture was warmed up to rt and stirred for 0.5 h, then cooled to –78 °C and iodopentane was added (0.45 mL, 3.5 mmol), the mixture was warmed up to rt, and stirred for 1 h. Dry DME (10 mL) was added, the mixture was cooled to –78 °C and n-BuLi (3.8 mmol) was added. After 15 min the mixture was allowed to warm to rt, stirred for 0.5 h, cooled to 0 °C and dry CuI (0.73 g, 3.8 mmol) was added. The mixture was stirred at rt for 1 h and pyridine (2.1 mL, 26 mmol) was added followed by 4-iodonitrobenzene (0.872 g, 3.50 mmol) and the mixture was gently refluxed for 20 hr. 10% HCl was added, organic products were extracted (CH_2Cl_2), extracts were dried (Na_2SO_4), solvents were evaporated and the residue was

separated by chromatography (SiO_2, hexane/CH_2Cl_2, 5:1) to give 250 mg (20% yield) of the desired product **6[A]** as the first fraction: mp 83.0-83.5 ^oC; ^1H NMR (400 MHz, $CDCl_3$) δ 0.84 (t, J = 7.3 Hz, 3H), 1.05-1.26 (m, 6H), 1.50-3.40 (m, 10H), 1.66 (br t, J = 8.3 Hz, 2H), 7.38 (d, J = 9.0 Hz, 2H), 8.02 (d, J = 9.0 Hz, 2H); ^{13}C NMR (125 MHz, $CDCl_3$) δ 13.8, 22.2, 29.1, 31.2, 38.0, 78.8 (br), 82.8 (br), 123.2, 128.4, 142.9, 147.6; ^{11}B NMR (128 MHz, $CDCl_3$) δ -12.2 (d, J = 164 Hz); IR (KBr) ν 2614 (B–H), 1598, 1514 (N–O), 1344 (N–O) cm^{-1}. Anal. Calcd for $C_{13}H_{25}B_{10}NO_2$: C, 46.55; H, 7.51; N, 4.18. Found: C, 46.79; H, 7.58; N, 4.27.

Acknowledgment

This work was supported by the NSF grant DMR-1207585.

References

1 R. N. Grimes *Carboranes*; Academic Press: London, 2011.
2 P. Kaszynski In *Boron Science: New Technologies & Applications*; Hosmane, N., Ed.; CRC Press: 2012, p 305-338.
3 P. Kaszynski, A. G. Douglass *J. Organomet. Chem.* 1999, **581**, 28-38.
4 P. Kaszynski, A. Januszko, K. L. Glab *J. Phys. Chem. B* 2014, **118**, 2238-2248.
5 L. Kobr, K. Zhao, Y. Shen, K. Polívková, R. K. Shoemaker, N. A. Clark, J. C. Price, C. T. Rogers, J. Michl *J. Org. Chem.* 2013, **78**, 1768-1777.
6 S. Körbe, P. J. Schreiber, J. Michl *Chem. Rev.* 2006, **106**, 5208-5249.
7 Y. Endo, T. Iijima, Y. Yamakoshi, H. Fukasawa, C. Miyaura, M. Inada, A. Itai *Chem. Biol.* 2001, **8**, 341-355.
8 T. Goto, K. Ohta, S. Suzuki, Y. Ohta, Y. Endo *Bioorg. Med. Chem.* 2005, **13**, 6414-6424.
9 B. T. S. Thirumamagal, X. B. Zhao, A. K. Bandyopadhyaya, S. Narayanasamy, J. Johnsamuel, R. Tiwari, D. W. Golightly, V. Patel, B. T. Jehning, M. V. Backer, R. F. Barth, R. J. Lee, J. M. Backer, W. Tjarks *Bioconjugate Chem.* 2006, **17**, 1141-1150.
10 A. W. Laubengayer, W. R. Rysz *Inorg. Chem.* 1965, **4**, 1513-1514.
11 A. I. Echeistova, Y. K. Syrkin, V. I. Stanko, A. I. Klimova *Russ. J. Struct. Chem.* 1967, **8**, 833-834.
12 P. Kirsch, M. Bremer *Angew. Chem. Int. Ed.* 2000, **39**, 4216-4235.
13 Handbook of Liquid Crystals, 2nd Ed; J. W. Goodby, Collings P. J.; Kato, T.; Tschierske, C.; Gleeson, H.; Raynes, P, Eds.; Wiley-VCH: New York, 2014.
14 B. Ringstrand, P. Kaszynski *J. Mater. Chem.* 2010, **20**, 9613-9615, and references therein.
15 J. Pecyna, B. Ringstrand, R. P. Denicola, H. M. Gray, P. Kaszynski *Liq. Cryst.* 2014, **41**, 1188–1198.
16 A. Jankowiak, P. Kaszynski *Inorg. Chem.* 2014, **53**, 8762−8769.
17 A. G. Douglass, S. Pakhomov, B. Both, Z. Janousek, P. Kaszynski *J. Org. Chem.* 2000, **65**, 1434-1441.
18 K. Czuprynski, A. G. Douglass, P. Kaszynski, W. Drzewinski *Liq. Cryst.* 1999, **26**, 261-269.
19 A. Januszko, K. L. Glab, P. Kaszynski, K. Patel, R. A. Lewis, G. H. Mehl, M. D. Wand *J. Mater. Chem.* 2006, **16**, 3183-3192.
20 R. A. Batey, M. Shen, A. J. Lough *Org. Lett.* 2002, **4**, 1411− 1414.
21 J. Y. Chang, J. H. Baik, C. B. Lee, M. J. Han, S.-K. Hong *J. Am. Chem. Soc.* 1997, **119**, 3197-3198.
22 J. Li, P. Huang *Beils. J. Org. Chem.* 2011, **7**, 426–431.
23 T. Nagamine, A. Januszko, K. Ohta, P. Kaszynski, Y. Endo *Liq. Cryst.* 2008, **35**, 865-884.
24 R. Coult, M. A. Fox, W. R. Gill, P. L. Herbertson, J. A. H. McBride, K. Wade *J. Organomet. Chem.* 1993, **462**, 19-29.
25 J. Newton, H. Walton, H. Colest, P. Hodges *Mol. Cryst. Liq. Cryst.* 1995, 107-125.
26 A. Merlo, A. Gallardo, T. R. Taylor, T. Kroin *Mol. Cryst. Liq. Cryst.* 1994, **250**, 31-39.
27 B. Priewisch, K. Rück-Braun *J. Org. Chem.* 2005, **70**, 2350–2352.
28 For details see the Electronic Supplementary Information.
29 R. Dabrowski, J. Dziaduszek, T. Szczucinski *Mol. Cryst. Liq. Cryst. Lett.* 1984, **102**, 155-160.
30 Z. Raszewski *Liq. Cryst.* 1988, **3**, 307-322.
31 W. Maier, G. Meier *Z. Naturforsch.* 1961, **16A**, 262-267 and 470-477.
32 Urban, S. in Physical Properties of Liquid Crystals: Nematics, D. A. Dunmur, A. Fukuda, and G. R. Luckhurst, Eds; IEE, London, 2001, pp 267-276.
33 L. I. Zakharkin, V. N. Kalinin, E. G. Rys *Bull. Acad. Sci. USSR, Div. Chem. Sci.* 1974, 2543-2545.
34 L. I. Zakharkin, V. N. Kalinin, I. P. Shepilov *Dokl. Akad. Nauk* 1967, **174**, 484EE.
35 P. T. Brain, J. Cowie, D. J. Donohoe, D. Hnyk, D. W. H. Rankin, D. Reed, B. D. Reid, H. E. Robertson, A. J. Welch *Inorg. Chem.* 1996, **35**, 1701-1708.
36 K. Toriyama, S. Sugimori, K. Moriya, D. A. Dunmur, R. Hanson *J. Phys. Chem.* 1996, **100**, 307-315.
37 B. Ringstrand, P. Kaszynski, A. Januszko, V. G. Young, Jr. *J. Mater. Chem.* 2009, **19**, 9204-9212.
38 H. Xianyu, S.-W. Wu, C.-L. Lin *Liq. Cryst.* 2009, **36**, 717-726.
39 M. Mrukiewicz, P. Perkowski, K. Garbat, R. Dabrowski *Liq. Cryst.* 2014, **41**, 1537-1544.
40 Gaussian 09, Revision A.02, M. J. Frisch, G. W. Trucks, H. B. Schlegel, G. E. Scuseria, M. A. Robb, J. R. Cheeseman, G. Scalmani, V. Barone, B. Mennucci, G. A. Petersson, H. Nakatsuji, M. Caricato, X. Li, H. P. Hratchian, A. F. Izmaylov, J. Bloino, G. Zheng, J. L. Sonnenberg, M. Hada, M. Ehara, K. Toyota, R. Fukuda, J. Hasegawa, M. Ishida, T. Nakajima, Y. Honda, O. Kitao, H. Nakai, T. Vreven, J. A. Montgomery, Jr., J. E. Peralta, F. Ogliaro, M. Bearpark, J. J. Heyd, E. Brothers, K. N. Kudin, V. N. Staroverov, R. Kobayashi, J. Normand, K. Raghavachari, A. Rendell, J. C. Burant, S. S. Iyengar, J. Tomasi, M. Cossi, N. Rega, J. M. Millam, M. Klene, J. E. Knox, J. B. Cross, V. Bakken, C. Adamo, J. Jaramillo, R. Gomperts, R. E. Stratmann, O. Yazyev, A. J. Austin, R. Cammi, C. Pomelli, J. W. Ochterski, R. L. Martin, K. Morokuma, V. G. Zakrzewski, G. A. Voth, P. Salvador, J. J. Dannenberg, S. Dapprich, A. D. Daniels, O. Farkas, J. B. Foresman, J. V. Ortiz, J. Cioslowski, and D. J. Fox, Gaussian, Inc., Wallingford CT, 2009.
41 M. Cossi, G. Scalmani, N. Rega, V. Barone *J. Chem. Phys.* 2002, **117**, 43-54 and references therein.
42 A. Januszko, P. Kaszynski, B. Gruner *Inorg. Chem.* 2007, **46**, 6078-6082.

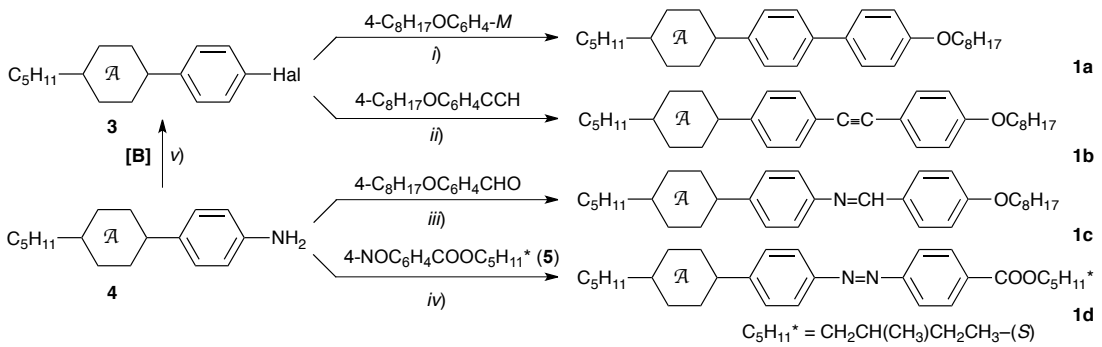

Scheme 1. Synthesis of **1**. Reagents and conditions: *i*) **[A]**: Hal = Br, *M* = $B(OCH_2)_2$, $Pd(PPh_3)_4$, Na_2CO_3, benzene, reflux (ref. [18]); **[B]**: Hal = Br, *M* = ZnCl, $Pd(dba)_2$, $PChx_3$, THF, reflux (ref. [16]); **[Ph]**: Hal = I, *M* = MgBr, $NiBr_2$, THF, reflux (ref. [18]); *ii*) Hal = I, $(i\text{-Pr})_2EtN$, $Pd(PPh_3)_2Cl_2$, CuI, THF, rt; *iii*) EtOH, cat. AcOH, reflux; *iv*) **[A]** and **[C]**: CH_2Cl_2, cat. AcOH, rt; **[B]**: AcOH, rt; *v*) **[B]**, Hal = I: (1) $[NO]^+[PF_6]^-$ and (2) $[Bu_4N]^+[I]^-$, MeCN, 0 °C (ref. [16]).

Table 1. Transition temperatures (°C) for **1**. [a]

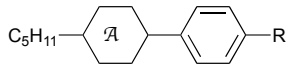

1

	R	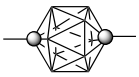 **A**	 **B**	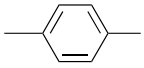 **Ph**
a	$–C_6H_4-OC_8H_{17}$	Cr 71 (SmA 45) N 149 I [b]	Cr 58 (SmC 38) SmA 121 N 144 I [c]	Cr 97 E 194 SmB 211 SmA 222 I [b]
b	$–C{\equiv}CC_6H_4-OC_8H_{17}$	Cr 90 N 176 I	Cr 114 SmA 140 N 168 I	Cr 96 Cr 156 B 177 N 206 I
c	$–N{=}CHC_6H_4-OC_8H_{17}$	Cr 111 N 177 I	Cr 101 SmA 157 N 171 I	Cr 95 (H? 90) G 138 SmF 150 SmI 166 SmC 191 SmA 198 N 214 I
d	$–N{=}NC_6H_4-COOC_5H_{11}^*$	Cr 94 N* 160 I	Cr 124 N* 151 I	Cr <25 E 115 SmB 136 SmA* 193 I

[a] Enthalpies are reported in the ESI. Cr-crystal, N-nematic, Sm-smectic, soft-crystalline phases B, E and G. [b] Ref [18]. [c] Ref. [16]

Table 2. Transition temperatures (°C) and enthalpies (kJ/mol, in italics) for **2**. [a]

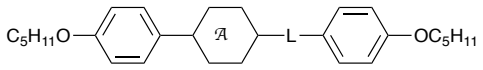

2

	L	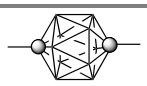 **A**	 **B**	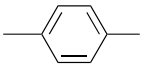 **Ph**
e	–CH=CH–	Cr 124 N 135 I [b]	Cr 121 (N 101) I [c]	Cr 72 X 209 G 254 SmC 258 SmA 281 N 285 I [b]
f	$–CH_2CH_2–$	Cr 94 N 123 I [b]	Cr 81 (N 78) I	Cr 118 B[d] 173 I [b]

[a] Enthalpies are reported in the ESI. Cr-crystal, N-nematic, Sm-smectic, soft-crystalline phases B and G, X-unidentified phase. [b] Ref [23]. [c] Ref. [16]. [d] Previously an E phase was reported.

TOC

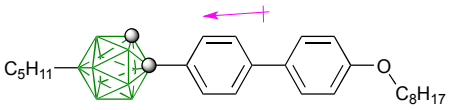

Cr 58 (SmC 38) SmA 121 N 144 I

μ = 8.75 D, β = 19.6°, $\Delta\varepsilon$ = 11.0, S_{app} = 0.60

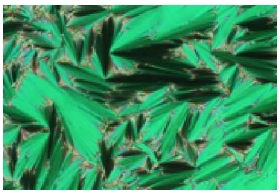

o-Carborane derivatives for probing molecular polarity effects on liquid crystal phase stability and dielectric behavior†

Jacek Pecyna,[a,b] Aleksandra Jankowiak,[a] Damian Pociecha,[c] and Piotr Kaszyński*[a,b,d,e]

Receipt/Acceptance Data **[DO NOT ALTER/DELETE THIS TEXT]**
Publication data **[DO NOT ALTER/DELETE THIS TEXT]**
DOI: 10.1039/b000000x [DO NOT ALTER/DELETE THIS TEXT]

A series of mesogenic derivatives of *o*-carborane was synthesized, their properties were analyzed by thermal, optical and XRD methods, and results were compared with those of isostructural *p*-carborane and benzene analogues. Comparative analysis revealed lower nematic phase stability and enhanced smectic behavior, including SmC, in the *o*-carborane derivatives relative to the isosteric *p*-carborane analogues. The effect of *o*-carborane on electrooptical properties was assessed for biphenyl derivative **1[B]a** in **6CHBT** nematic host giving the extrapolated $\Delta\varepsilon$ = 11.0, and a moderate increase of elastic constants K_{ii}. Complete analysis of dielectric results for *o*-carborane and *p*-carborane analogues **1[B]a** and **1[A]a** with the Maier-Meier formalism was augmented with DFT computational methods.

Introduction

During the past two decades *para*-carborane,[1] [*closo*-1,12-$C_2B_{10}H_{12}$] (**A**, Fig. 1), has become an attractive linear structural element of liquid crystals,[2-4] molecular construction sets,[5,6] and pharmacological compounds,[7-9] owing primarily to its geometry, symmetry, and chemical reactivity. In contrast, the two isomers of **A**, *ortho*-carborane (**B**) and *meta*-carborane (**C**) received much less attention, even though they have additional properties that are of particular interest for certain molecular and functional designs. For instance, in contrast to **A**, *ortho*- and *meta*-carboranes have ground-state dipole moments of 4.53 D and 2.85 D, respectively,[10,11] which are oriented about 30° to the 1,12-axis for **B** and nearly parallel to the 2,9- axis in **C** (Fig. 1). The different magnitude and orientation of the molecular dipole moment in the three essentially isosteric carboranes are of interest for fundamental studies of the liquid crystal phenomenon and for developing of materials for LCD applications.[12,13] One such a fundamental question relates to the role of the molecular electric dipole in smectic phase induction and liquid crystalline phase stabilization in general.[14,15] A comparison of properties of isosteric mesogenic derivatives **IA** – **IC** would provide an opportunity for such investigation, and also for the development of new polar materials for electrooptical applications.

Recently, we have reported practical access to isomerically pure 1,12-difunctionalized derivatives of *o*-carborane,[16] which opened up the door to investigation of new classes of liquid crystals of type **IB**. In this context two such derivatives, **1[B]a** and **2[B]e** (Fig. 2) were prepared and their preliminary studies indicated a significant smectogenic character,[16] which warrants further detailed investigation. Here we describe synthesis and characterization of a series of isostructural derivatives **1** and **2** (Fig. 2) in which isosteric carborane derivatives of type **IA** and **IB** are compared to those of benzene analogues. The smectic phases are analyzed by powder XRD and selected derivatives are investigated by dielectric methods as low concentration

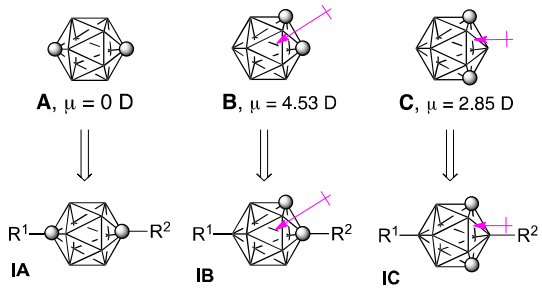

Fig 1. The structures of three isomeric carboranes [*closo*-$C_2B_{10}H_{12}$], **A**, **B** and **C**, and their disubstituted derivatives **IA**, **IB**, and **IC**, respectively. Each vertex represents a BH fragment and the sphere is a carbon atom. The arrow represents the electric dipole vector of the cluster (values from ref [10]).

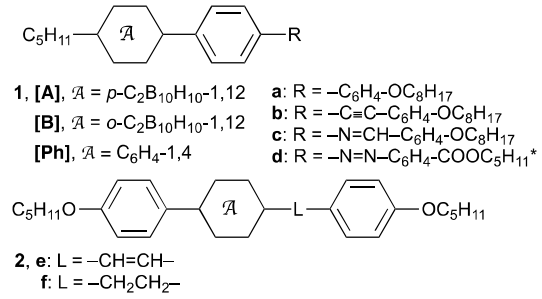

Fig. 2. The structures of investigated compounds. Definitions of rings **A** and **B** are shown in Fig. 1.

[a] *Department of Chemistry, Vanderbilt University, Nashville, TN 37235, USA, Tel: 1-615-322-3458; E-mail: piotr.kaszynski@vanderbilt.edu.*
[b] *Department of Chemistry, Middle Tennessee State University, Murfreesboro, TN 37132, USA.*
[c] *Department of Chemistry, University of Warsaw, Zwirki i Wigury 101, 02-089 Warsaw, Poland.*
[d] *Faculty of Chemistry, University of Łódź, Tamka 12, 91-403 Łódź, Poland.*
[e] *Centre of Molecular and Macromolecular Studies, Polish Academy of Sciences, Sienkiewicza 112, 90-363 Łódź, Poland.*

† Electronic Supplementary Information (ESI) available: details of thermal and dielectic analysis of binary mixture, additional XRD data, partial results of DFT calculations, archive of equilibrium geometries for **1[A]a** and **1[B]a**. This material is available free of charge via the Internet at http://pubs.acs.org. See http://dx.doi.org/10.1039/b000000x/

additives in a nematic host. Experimental results are augmented with DFT calculations and dielectric data are analyzed by the Maier-Meier formalism.

Results

Synthesis

Biphenyls **1a** were obtained from appropriate haloarenes **3** in C–C cross-coupling reactions with 4-$C_8H_{17}OC_6H_4M$ (Scheme 1): Suzuki for **1[A]a** (Hal = Br,[17] M = $B(OCH_2)_2$),[18] Negishi for **1[B]a** (Hal = I, M = ZnCl),[16] and Kumada for **1[Ph]a** (Hal = I,[19] M = MgBr),[18] and their details are described elsewhere. The iodoarenes **3** (Hal = I) were also used for a modified Sonogashira[20] coupling reaction with 4-$C_8H_{17}OC_6H_4CCH$[21,22] and preparation of tolanes **1b** (Scheme 1); the corresponding bromides were ineffective in this reaction. The reaction was conducted at ambient temperature in the presence of anhydrous non-nucleophilic Hunig's base to avoid amine- and hydroxide-promoted deboronation of *o*-carborane derivatives.

Anilines **4[A]**, **4[B]**,[16] and **4[Ph]** [5] served as suitable precursors to Schiff bases **1c** and azobenzene derivatives **1d** obtained by acid-catalyzed condensation with 4-$C_8H_{17}OC_6H_4CHO$ and 4-nitrosobenzoate ester **5**, respectively (Scheme 1). Aniline **4[B]** was also converted to the corresponding iodide **3[B]** (Hal = I) by a modified Sandmeyer reaction,[16] while iodide **3[A]** (Hal = I) was obtained by transhalogenation of the analogous bromide[17] **3[A]** (Hal = Br, *n*-BuLi followed by I_2).

SCHEME 1

Dimethylene-linked derivatives **2f** were obtained by Pd-catalyzed hydrogenation[23] of the previously reported stilbenes **2e**,[16,23] as shown for **2[B]f** in Scheme 2.

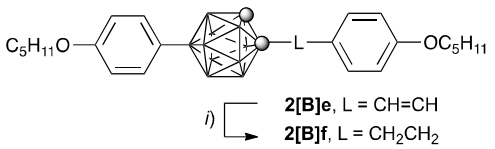

Scheme 2. Synthesis of liquid crystal **2[B]f**. Reagents and conditions: *i*) H_2 (50 psi), Pd/C (10%), THF, rt.

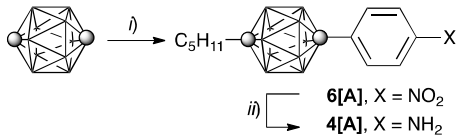

Scheme 3. Synthesis of aniline **4[A]**. Reagents and conditions: *i*) 1. *n*-BuLi, THF, –78 °C→0 °C; 2. *n*-$C_5H_{11}I$, –78 °C→rt; 3. DME, *n*-BuLi, –78 °C→rt; 4. CuI, 0 °C; 5. Pyridine; 6. 4-$IC_6H_4NO_2$, reflux; *ii*) H_2 (40 psi), Pd/C (10%), THF, rt.

The preparation of aniline derivative of *p*-carborane **4[A]** is shown in Scheme 3. The first step is a one-pot alkylation–arylation[24] process, which gave the desired nitrophenyl derivative **6[A]** in 20% yield after careful chromatographic separation from several by-products. Subsequent catalytic reduction of **6[A]**, as described for **6[B]**,[16] gave aniline **4[A]**.

The nitroso ester **5** was prepared by partial oxidation of the known[25,26] 4-aminobenzoate ester **7** with Oxone®, according to a general literature procedure[27] (Scheme 4).

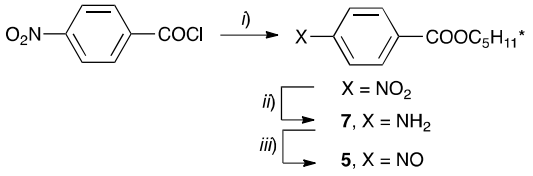

Scheme 4. Synthesis of nitroso ester **5**. Reagents and conditions: *i*) (*S*)-2-methylbutan-1-ol, pyridine; *ii*) H_2 (40 psi), Pd/C (10%), THF, rt; *iii*) Oxone®, CH_2Cl_2/H_2O, rt.

Thermal analysis

Transition temperatures and enthalpies of compounds **1** and **2** were determined by differential scanning calorimetry (DSC). Phase structures were assigned by optical microscopy in polarized light and confirmed by powder XRD measurements. The results are shown in Tables 1 and 2 and Fig. 3–5.

All carborane derivatives in series **1** form a nematic phase with clearing temperatures in a range of 78–177 °C, while smectic phases were found only in **1[A]a**, **1[B]a**–**1[B]c** (Table 1, Fig. 3 and 4). Compounds **2[B]e** and **2[B]f** have the lowest T_{NI} in the series and are the only compounds with monotropic behavior. Surprisingly however, crystalline polymorphs obtained from melt have significantly lower melting points (63 °C [16] and 69 °C, respectively) and the nematic phase becomes enantiotropic for both compounds. Such a large difference in melting temperatures of crystalline polymorphs (ΔT = 58 K for **2[B]e**) is rarely observed for mesogens and never before for carborane derivatives.

TABLES 1 and 2

Comparative analysis demonstrates that *o*-carborane derivatives **1[B]** have lower clearing temperatures (T_c) and higher smectogenic character than the *p*-carborane analogues **1[A]**. For the first four members of the series, **1a**–**1d**, the difference in T_c is small (average ΔT_c = 7±2 K; Table 1, Fig. 5), while the difference for the pairs **2e** and **2f** is significantly greater (14 K and 23 K, respectively; Table 2). This decrease of phase stability upon substitution of *o*-carborane for *p*-carborane indicates the importance of increased lateral dipole–dipole interactions and arising from them relative difficulties in molecular packing in the mesophase particularly for **2[B]e** and **2[B]f** in which the bulky carborane unit is in the center of the rigid core. This corroborates with the observed significant increase of smectogenic behavior upon replacement of *p*-carborane with the isosteric *o*-carborane. Thus, a SmA phase is more stable by 76 K in **1[B]a**, than in the *p*-carborane analogue **1[A]a**, and in compounds **1b** and **1c** this stabilization is at least 45 K (Table 1). Moreover, a monotropic SmC phase was also detected in **1[B]a** (Fig. 4c).

Although *o*-carborane derivatives have relatively strong tendency to the formation of lamellar phases, this behavior is far from the smectogenic character of the benzene analogues **1[Ph]**. For instance, SmA phase is more stable by over 100 K in **1[Ph]a** than in **1[B]a**, and Schiff base **1[Ph]c** and stilbene

1[Ph]e exhibit rich smectic polymorphism (Tables 1 and 2). This observed difference in smectogenic behavior is related to the shape of the carborane and benzene and, consequently, to molecular packing of their derivatives in lamellar phases, as it was already postulated for *p*-carborane derivatives.[2] Interestingly, chiral azo ester **1[Ph]d** does not crystallize and exhibits an E phase at ambient temperature (Fig. 4d).

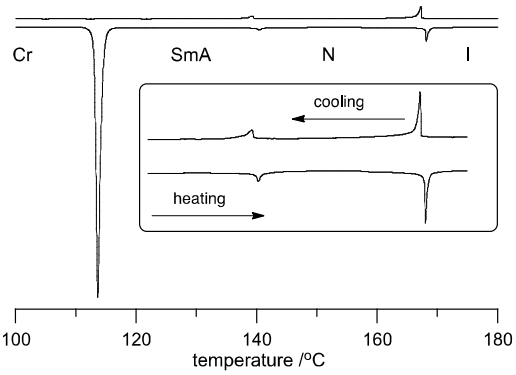

Fig. 3. DCS trace for **1[B]b**; heating rate 5 K min^{-1}. The inset shows a magnified portion of the trace with the SmA–N and N–I transitions.

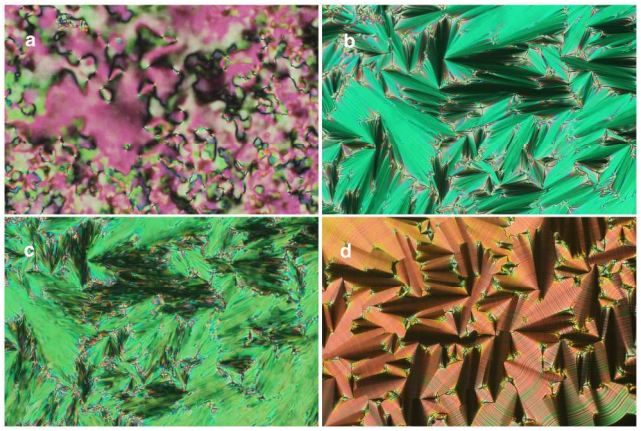

Fig. 4. Optical textures obtained by cooling from the isotropic phase of **1[B]a**: a) N (135 °C), b) SmA (100 °C) and c) SmC phase (30 °C), and of **1[Ph]d**: d) E phase (100 °C).

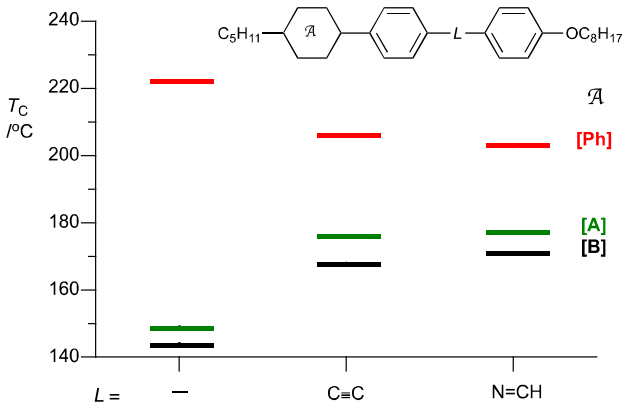

Fig. 5. Trends in mesophase stability (N–I or SmA–I transition temperatures) as a function of the linking group *L* in series **1**.

Series **1a**–**1c** permitted an analysis of the impact of the linking group *L* on mesophase stability. Thus, insertion of a two-atom fragment between the benzene rings in the terphenyl derivative **1[Ph]a** lowered the mesophase stability in **1[Ph]b** and **1[Ph]c** by nearly 20 K (Fig. 5) presumably due to increased flexibility of the core and lower packing fraction. In contrast, the analogous transformation of carborane derivatives **1[A]a** and **1[B]a** stabilized the nematic phase by about 25 K in the corresponding derivatives **1b** and **1c**. Also the SmA phase was significantly stabilized in the *o*-carborane derivatives **1[B]b** and **1[B]c** relative to **1[B]a**.

Molecular Modeling

For a better understanding of powder XRD results and the impact of substitution of *p*-carborane with *o*-carborane on molecular dimensions, molecular structures of selected compounds were fully optimized at the B3LYP/6-31G(2d,p) level of theory. Analysis of results demonstrated that the structurally analogous *o*-carborane and *p*-carborane derivatives are essentially isosteric with the total length of about 31 Å (for **1a**) or 33 Å (for **1b** and **1c**) in the most extended conformations (Fig. 6).[28] The benzene analogues are about 0.7 Å shorter than the corresponding carborane derivatives.

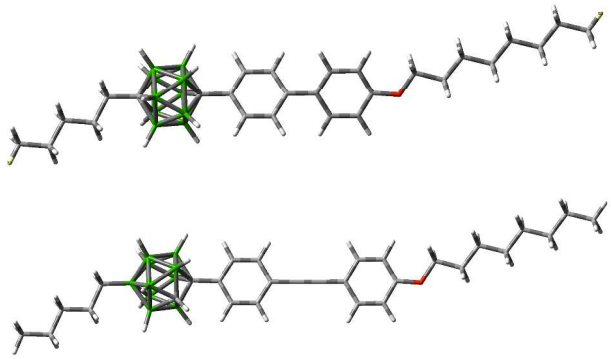

Fig. 6. Equilibrium geometry for **1[A]a** (upper) and **1[B]b** (lower) at the B3LYP/6-31G(2d,p) level of theory.

Powder XRD data

Analysis of smectic phases formed by *o*-carborane (**B**) derivatives revealed typical behavior: the layer thickness in SmA phase slightly increases with lowering temperature due to diminishing thermal motions (e.g. $\kappa = -9.65\pm0.08$ pm K^{-1} for **1[B]b**), while the SmC layer in **1[B]a** contracts rapidly due to the progression of the molecular tilt.[28] The observed interlayer spacing in the SmA phase is about 2 Å shorter than the calculated molecular lengths.

XRD analysis of benzene derivatives **1[Ph]a** – **1[Ph]c** confirmed their rich smectic polymorphism, as shown for **1[Ph]c** in Fig. 7. Thus, below SmA and SmC phases, there are more organized tilted smectic (SmI, SmF) and soft crystalline phases with transitions well marked by the changes of intensity of the diffraction signal related to the layer thickness. Phase identification was confirmed by analysis of the wide angle range of XRD patterns.[28] The transition from the SmC having liquid-like layers to a hexatic SmI is accompanied by a relatively large enthalpy of transition (3.6 kJ mol^{-1}), which is consistent with increasing positional correlations of molecules within the smectic layers. The measured layer spacing in the SmA phase is 32.3 Å, which correlated well with the calculated

molecular length of 32.4 Å. Similar analysis was performed for other benzene derivatives and details are listed in the ESI.

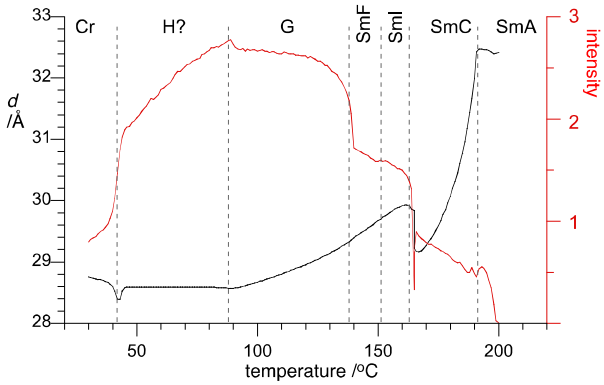

Fig. 7. Layer spacing *d* and intensity of related XRD signal for **1[Ph]c** as a function of temperature.

XRD analysis of **2[Ph]f** revealed a soft crystalline B phase instead of an E phase, which was previously reported[23] on the basis of microscopic observations.

Binary mixtures

To assess the impact of the molecular dipole moment of *o*-carborane on electrooptical properties, two isostructural biphenyls **1[A]a** and **1[B]a** were investigated as low concentration additives to **6CHBT**,[28-30] which is an ambient temperature nematic characterized by a positive Δε = +8.06.

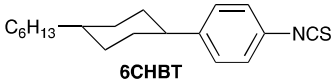

Thermal analysis of the binary mixtures demonstrated a linear dependence of the nematic-isotropic transition on concentration for the *p*-carborane derivative **1[A]a**, while the correlation for the *o*-carborane analogue **1[B]a** deviates from the linearity above 10 mol% (Fig. 8). Linear extrapolation of the mixture's N–I transition peak temperatures to the pure additive gave the virtual N–I transition temperatures [T_{NI}] of 187±3 °C for **1[A]a** and 148±3 °C for **1[B]a** in **6CHBT**. A comparison of the clearing temperatures for pure compounds (Table 1) with the extrapolated values [T_{NI}] demonstrates that the nematic phase of *p*-carborane **1[A]a** is stabilized by nearly 30 K in the host relative to the pure compound. Additional stabilization of the nematic phase is also apparent for **1[B]a** at higher concentrations (Fig. 8); however at concentrations <10 mol% the the mixture exhibits nearly ideal behavior.

Dielectric analysis of the binary mixtures in **6CHBT** at 1 kHz revealed linear dependence of dielectric parameters on concentration (Fig. 9), which, after extrapolation, established dielectric values shown in Table 3. As expected, the polar derivative **1[B]a** has a substantial longitudinal dielectric permittivity component $\varepsilon_{||}$ = 17.5 and, consequently, a significant positive dielectric anisotropy Δε = 11.0. In contrast, the *p*-carborane analogue **1[A]a** has a small negative Δε = –1.1, resulting from unrealistically low $\varepsilon_{||}$ = 0.2.

The carborane additives also affect elastic constants of the host: both compounds systematically increase splay and twist constants K_{11} and K_{22}, although the effect is smaller for the *o*-carborane derivative **1[B]a**. For instance both values are higher by about 30% for 10 mol% solutions. Further analysis indicates that the *p*-carborane derivative **1[A]a** lowers the rotational viscosity of the host, while the results for the **1[B]a** analogue are ambiguous.

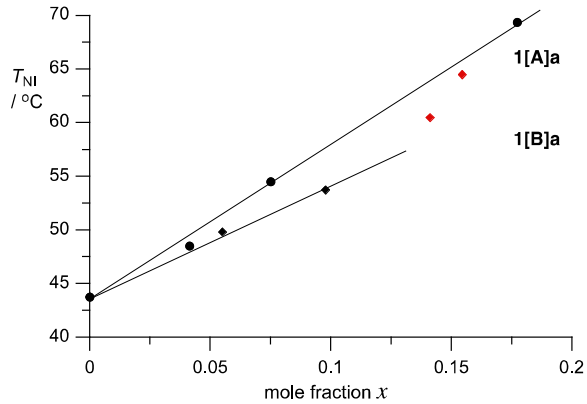

Fig. 8. A plot of peak temperature of the N–I transition for binary mixtures of **1[A]a** (circles) and **1[B]a** (diamonds) in **6CHBT**.

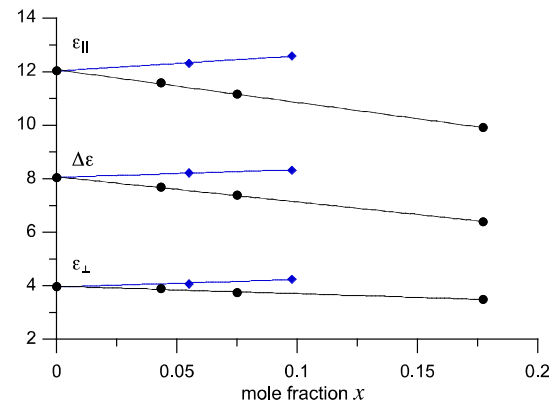

Fig. 9. Dielectric parameters of binary mixtures of **1[A]a** (black) and **1[B]a** (blue) in **6CHBT** as a function of concentration.

Table 3. Extrapolated experimental (upper) and predicted (lower) dielectric data and results of Maier-Meier analysis for **1[A]a** and **1[B]a**. [a]

Compd		$\varepsilon_{\parallel}$	$\varepsilon_{\perp}$	Δε	S_{app}	g
1[A]a	exp	0.2	1.3	-1.1	0.45	-2.06
	theory	5.0[b]	3.5[b]	1.5[b]	0.67[c]	0.45[c]
1[B]a	exp	17.5	6.5	11.0	0.60	0.28
	theory	26.9[b]	7.9[b]	19.0[b]	0.67[c]	0.45[c]

[a] For details see text and the ESI. Typical error of extrapolated dielectric parameters is ±0.20. [b] Calculated value assuming host's order parameter S = 0.67 and g = 0.45. [c] Assumed values.

Analysis of dielectric data

Dielectric parameters extrapolated for pure additives were analyzed using the Maier-Meier relationship (eq 1),[31,32] which connects molecular and phase parameters. Using experimental $\varepsilon_{\parallel}$ and Δε values (Table 3) and DFT-calculated parameters μ, α, and β (Table 4), equations 2 and 3 permitted the calculation of the apparent order parameter S_{app} and the Kirkwood factor $g = \mu^2_{eff}/\mu^2$ shown in Table 3. The effect of the additive was neglected and the field parameters F and h in equations 2 and 3 were calculated using the experimental dielectric and optical data for pure **6CHBT** host.[28-30]

$$\Delta\varepsilon = \frac{NFh}{\varepsilon_0}\left\{\Delta\alpha - \frac{F\mu_{eff}^2}{2k_BT}(1-3cos^2\beta)\right\} \quad \text{eq 1}$$

$$S_{app} = \frac{2\Delta\varepsilon\varepsilon_0}{NFh[2\Delta\alpha+3\bar{\alpha}(1-3cos^2\beta)]-3(\bar{\varepsilon}-1)\varepsilon_0(1-3cos^2\beta)} \quad \text{eq 2}$$

$$g = \frac{[(\varepsilon_{\parallel}-1)\varepsilon_0-\bar{\alpha}NFh-\frac{2}{3}\Delta\alpha NFhS_{app}]3k_BT}{NF^2h\mu^2[1-(1-3cos^2\beta)S_{app}]} \quad \text{eq 3}$$

Molecular electric dipole moment μ and polarizability α required for the Maier-Meier analysis of dielectric results were obtained at the B3LYP/6-31+G(2d,p)//B3LYP/6-31G(2d,p) level of theory in the dielectric medium of the host.[28]

Table 4. Calculated molecular parameters for **1[A]a** and **1[B]a**. [a]

Compd	$\mu_{\parallel}$ /D	$\mu_{\perp}$ /D	μ /D	β[b] /°	Δα /Å^3	α_{avrg} /Å^3
1[A]a	1.63	1.12	1.98	34.5	48.2	84.6
1[B]a	8.24	2.93	8.75	19.6	49.9	85.3

[a] Obtained at the B3LYP/6-31+G(2d,p)// B3LYP/6-31G(2d,p) level of theory in **6-CHBT** dielectric medium. For details see text and the ESI. [b] Angle between the net dipole vector μ and $\mu_{\parallel}$.

Data in Table 4 demonstrate that the replacement of *p*-carborane with *o*-carborane increases particularly strongly the longitudinal dipole moment component. The modest dipole moment of *p*-carborane derivative **1[A]a**, μ = 1.98 D, results from a combination of mainly two local dipole moments associated with the weakly polar alkoxyphenyl group and polarization from the electron-donating alkoxy group to the electron withdrawing carborane unit (σ_p = 0.12).[33] The resulting net dipole is oriented at 34.5° relative to the molecular axis of inertia. Substitution of the *o*-carborane for *p*-carborane in **1[A]a** increases polarization of the rigid core in **1[B]a** due to a higher electron-withdrawing character of the cluster (σ_p = 0.43)[34] and also introduces a reinforcing additional local dipole associated with the cage itself (Fig. 10). This results in a substantial longitudinal dipole moment component, $\mu_{\parallel}$ = 8.24 D, and a smaller angle β ≈ 20° (Table 4). Thus, on the basis of the calculated molecular dipole moment it is expected that the *p*-carborane derivative **1[A]a** will exhibit a small positive value of dielectric anisotropy, Δε = 1.5, while the *o*-carborane **1[B]a** will possess a significant Δε = 19.0, assuming host's order parameter *S* = 0.67 and a reasonable Kirkwood factor *g* = 0.45 (Table 3). Experimental dielectric values are, however, significantly smaller.

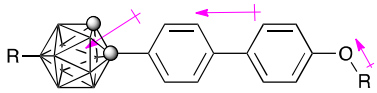

Fig. 10. Major local dipole moments in **1[B]a**.

Experimental data in Table 3 show that the dielectric parameters for **1[B]a** are smaller than expected, especially the $\varepsilon_{\parallel}$ component (17.5 instead of 26.9). Consequently, the calculated apparent order parameter S_{app} is lower than that for the host, and the Kirkwood factor *g* is unusually small (0.28) at concentrations <10 mol%; the latter parameter may indicate significant aggregation in the solution, while the S_{app} suggests poor alignment of the molecules (presumably aggregates) in the nematic phase. The dielectric results for the *p*-carborane analogue **1[A]a** are more difficult to rationalize: while the low value of S_{app} is small but acceptable, the negative *g* factor is physically unrealistic, although consistent with the unrealistically low extrapolated $\varepsilon_{\parallel}$ = 0.2 (predicted 5.0, Table 3). Similar results were obtained for solutions of another *p*-carborane derivative in **6CHBT**,[19] which presumably reflect molecular dynamics at 1 kHz and specific solute-solvent interactions. In all cases, the unusually low extrapolated $\varepsilon_{\parallel}$ results in excessively negative extrapolated Δε values.

Discussion

The recent availability[16] of isomerically pure derivatives **8** and **9** opened the way to a new class of polar mesogens based on *o*-carborane (Fig. 11). In general, these currently available precursors permit incorporation of motifs **I** and **II** into the molecular structure as either a terminal or central part of the rigid core. Thus far, the B(12)–I group was used for B-alkylation (Negishi pentylation of **8**) and B-arylation (pentyloxyphenylation of **9**) reactions, and the vinyl group in **9** was arylated in the Heck coupling,[16] however other C–C coupling reactions and synthesis of other intermediates are possible to expand the structural variety and fine-tuning of molecular and bulk properties of the materials. The first series of *o*-carborane-containing mesogens presented here was obtained using mainly 4-halophenyl derivatives **3[B]** and aniline **4[B]**, which can serve as versatile precursors to other similar mesogenic derivatives.

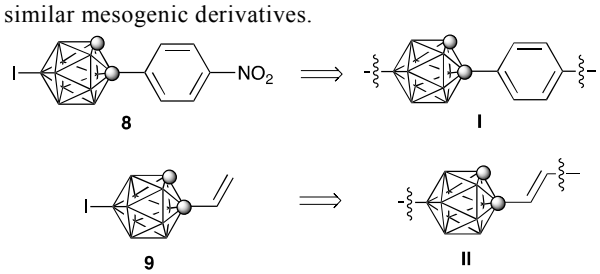

Fig. 11. Precursors **8** and **9** derived from them molecular fragments **I** and **II**.

Results for the handful of available mesogenic *o*-carborane derivatives demonstrate that compounds containing fragment **I** (series **1[B]**) exhibit greater propensity to the formation of smectic phases than those in series **2[B]**. This is presumably because of the position of the bulky carborane unit in the molecule: in **1[B]** it resides at the edge of the rigid core, which is more favorable for the formation of lamellar phases further enhanced by lateral dipole-dipole interactions.

A comparison of mesogenic derivatives of *o*-carborane with the isosteric *p*-carborane analogues provides an excellent opportunity for a better understanding of the fundamental issue of the role of a molecular dipole moment in phase stability. In recent years, we have demonstrated that replacement of the non-polar C–C bond in carborane derivatives with the isosteric polar B–N bond introduces a substantial longitudinal dipole moment of 12 D in 10-vertex and 10 D in 12-vertex derivatives.[14,15] This replacement generally increases the nematic phase stability by up to 55 K, and, surprisingly, does not induce smectic polymorphism. In the present work, we compare isomeric carborane derivatives, which result from the exchange of positions of cluster's B and C atoms. The results

show that phases formed by the polar *o*-carborane derivatives are less thermodynamically stable and smectic polymorphism is more pronounced, when compared to the weakly polar *p*-carborane analogues. The compounds are essentially isosteric but conformational properties of the carborane–aryl(alkyl) bond differ somewhat due to the relatively short C–C bond in *o*-carborane. This is evident from the analysis of molecular models for **1[B]** and consistent with experimental data for 1-phenyl-*o*-carborane[35] (Fig. 12).

Fig. 12. A pseudo-Newman projection of a conformational minimum of 1-phenyl-*o*-carborane (ref[35]). The bar represents the benzene ring plane and the spheres are the carbon atoms.

Dielectric data for the two carborane derivatives **1[A]a** and **1[B]a** show smaller than expected $\varepsilon_{\parallel}$ components (hence lower $\Delta\varepsilon$ values), presumably due to specific polar solvent – polar solute interactions,[36] molecular aggregation,[37] and/or molecular dynamics; the former depend on the host, while the dynamics on the frequency used in the measurement. If the low $\varepsilon_{\parallel}$ value is due mainly to the frequency of the oscillating electric field (which is plausible especially for the weakly polar **1[A]a**), then both compounds may exhibit a low cross-over frequency f_c (where $\Delta\varepsilon$ changes the sign) just above the measuring frequency (1 kHz). In such a case, compounds of this type, in which there is a large heavy substituent (the carborane cage) at the end of the rigid core with a significant moment of inertia, are potentially suitable for formulation of materials for dual-frequency addressing of LC displays.[38,39] This warrants further detailed investigation of such derivatives with dielectric spectroscopy tools.

Summary and Conclusions

A strategy to a potentially broad series of liquid crystalline derivatives of the polar *o*-carborane has been developed and demonstrated on a handful of derivatives. These derivatives exhibit somewhat lower clearing temperatures and higher smectic phase stability than the analogous derivatives of *p*-carborane. The inherent dipole moment of *o*-carborane cage gives rise to a substantial molecular dipole moment oriented along the main axis, which results in sizable dielectric anisotropy ($\Delta\varepsilon$ = 11.0 in **6CHBT** host at 1 kHz) and makes such derivatives attractive for electrooptical applications. Also the combination of smectogenic character and inherent polarity of *o*-carborane derivatives is of interest for the development of materials for FLC and AFLC applications. Initial results also suggest that derivatives of type **1** may have a relatively low cross-over frequency f_c and thus may be attractive for dual-frequency devices. These results warrant further exploration of mesogenic carborane derivatives as additives to nematic and smectic hosts.

Computational Details

Quantum-mechanical calculations were carried out using Gaussian 09 suite of programs.[40] Geometry optimizations for unconstrained conformers of **1a** with most extended molecular shapes were undertaken at the B3LYP/6-31G(2d,p) level of theory using default convergence limits. Vibrational frequencies were used to characterize the nature of the stationary points and to obtain exact polarizabilities in vacuum. The alkyl groups were in all-*trans* conformation. No conformational search was attempted. Final coordinates for each molecular model are provided in the ESI.

Dipole moments and exact electronic polarizabilities of **1a** used in the Maier–Meier data analysis were obtained in **6CHBT** dielectric medium using the B3LYP/6-31+G(2d,p)// B3LYP/6-31G(2d,p) method and the PCM solvation model[41] requested with SCRF(Solvent=Generic, Read) keywords and "eps=6.70" and "epsinf=2.4623" parameters (single point calculations). Exact polarizabilities were obtained using the POLAR keyword. The reported values for dipole moment components and dielectric permittivity tensors are at Gaussian standard orientation of each molecule (charge based), which is close to the principal moment of inertia coordinates (mass based), are listed in the ESI.

Experimental Section

General. NMR spectra were obtained at 400.1 MHz (^{1}H), 125 MHz (^{13}C), and 128.4 MHz (^{11}B), using a 9.4 T Bruker or JOEL ECX 500 instrument in $CDCl_3$, unless specified otherwise. ^{1}H NMR spectra were referenced to the solvent and ^{11}B NMR chemical shifts to an external boric acid sample in CH_3OH that was set to 18.1 ppm. Thermal analysis was obtained using a TA Instruments DSC 2920 using small samples of about 0.5-1.0 mg. IR spectra were recorded in KBr pellets using ATI Mattson Infinity FTIR 60. HRMS data were obtained on a Bruker micrOTOF II instrument. MALDI-TOF mass data were acquired using a Voyager Elite instrument.

Binary mixtures preparation. Solutions of carborane derivatives **1a** in **6CHBT** host (15-20 mg of the host) were prepared in an open vial. A mixture of the compound and the host in CH_2Cl_2 was heated for 2 hr at 60 ^{o}C to remove the solvent and evacuated (10^{-2} Torr). The resulting binary mixtures were analyzed by polarized optical microscopy (POM, PZO Biolar) to ensure homogeneity. The mixtures were then allowed to stand for 2 hr at room temperature before thermal and dielectric measurements.

Electrooptical measurements. Dielectric properties of solutions of selected compound in **6CHBT** were measured by a Liquid Crystal Analytical System (LCAS - Series II, LC Vision, Inc.) using GLCAS software version 0.13.14, which implements literature procedures for dielectric constants. The instrument was calibrated using a series of capacitors. The homogenous binary mixtures were loaded into ITO electro-optical cells by capillary forces with moderate heating supplied by a heat gun. The cells (about 10 μm thick, electrode area 1.00 cm^2 and anti-parallel rubbed polyimide layer) were obtained from LC Vision, Inc. The filled cells were heated to an isotropic phase and cooled to rt before measuring the dielectric

properties. Default parameters were used for measurements: triangular shaped voltage bias ranging from 0.1-20 V at 1 kHz frequency. The threshold voltage V_{th} was measured at a 5% change. For each mixture the measurement was repeated 10 times manually for two cells. The results were averaged to calculate the mixture's parameters. Results are provided in ESI and extrapolated values for pure additives are shown in Table 3.

Preparation of derivatives of tolanes 1b. General procedure. To a solution of 4-octyloxyphenylacetylene[21,22] (0.35 mmol), iodoarene **3** (0.30 mmol) in dry THF (3 mL) and Hunig's base (0.2 mL) were added at rt under Ar atmosphere, followed by $Pd(PPh_3)_2Cl_2$ (0.03 mmol) and CuI (0.015 mmol). The mixture was stirred at rt for 2-3 h, 5% HCl was added, organic products were extracted (CH_2Cl_2), extracts dried (Na_2SO_4), and solvents were evaporated. The crude product was purified on a silica gel plug (CH_2Cl_2/hexane, 1:5) followed by repeated recrystallization (hexane and EtOH/EtOAc).

4-(12-C_5H_{11}-*p*-carboran-1-yl)$C_6H_4C{\equiv}CC_6H_4OC_8H_{17}$ (1[A]b). White solid: ^{1}H NMR (400 MHz, $CDCl_3$) δ 0.84 (t, *J* = 7.3 Hz, 3H), 0.88 (t, *J* = 6.8 Hz, 3H), 1.08-1.38 (m, 8H), 1.45 (quint, *J* = 7.4 Hz, 2H), 1.50-4.0 (m, 10H), 1.65 (br t, *J* = 8.4 Hz, 2H), 1.78 (quint, *J* = 7.1 Hz, 2H), 3.96 (t, *J* = 6.6 Hz, 2H), 6.84 (d, *J* = 8.8 Hz, 2H), 7.15 (d, *J* = 8.6 Hz, 2H), 7.27 (d, *J* = 8.6 Hz, 2H), 7.40 (d, *J* = 8.8 Hz, 2H); ^{13}C NMR (125 MHz, $CDCl_3$) δ 13.9, 14.1, 22.2, 22.6, 26.0, 29.16, 29.22, 29.33, 29.7, 31.2, 31.8, 37.9, 68.1, 80.5 (br), 81.6 (br), 87.0, 90.7, 114.5, 114.8, 123.7, 127.2, 130.9, 133.0, 135.9, 160.0; ^{11}B NMR (128 MHz, $CDCl_3$) δ -12.3 (d, *J* = 164 Hz); IR (KBr) ν 2607 (B–H), 2217 (C≡C), 1516, 1247 cm^{-1}; MALDI-TOF (ANP) *m/z* 516.5–521.5 (max at 519.5, $[M]^+$). Anal. Calcd for $C_{29}H_{46}B_{10}O$: C, 67.14; H, 8.94. Found: C, 67.15; H, 9.05.

4-(12-C_5H_{11}-*o*-carboran-1-yl)$C_6H_4C{\equiv}CC_6H_4OC_8H_{17}$ (1[B]b). White solid: ^{1}H NMR (400 MHz, $CDCl_3$) δ 0.73 (br t, *J* = 6.6 Hz, 2H), 0.87 (t, *J* = 6.6 Hz, 3H), 0.89 (t, *J* = 7.4 Hz, 3H), 1.20-1.39 (m, 14H), 1.50-4.0 (m, 9H), 1.45 (quint, *J* = 7.3 Hz, 2H), 1.77 (quint, *J* = 7.1 Hz, 2H), 3.90 (br s, 1H), 3.97 (t, *J* = 6.6 Hz, 2H), 6.86 (d, *J* = 8.8 Hz, 2H), 7.41-7.48 (m, 6H); MALDI-TOF (CHCA) *m/z* 516.5–521.5 (max at 519.5, $[M]^+$). Anal. Calcd for $C_{29}H_{46}B_{10}O$: C, 67.14; H, 8.94. Found: C, 67.07; H, 8.93.

4-(12-C_5H_{11}-C_6H_4)$C_6H_4C{\equiv}CC_6H_4OC_8H_{17}$ (1[Ph]b). White solid: ^{1}H NMR (400 MHz, CD_2Cl_2) δ 0.90 (t, *J* = 7.0 Hz, 3H), 0.91 (t, *J* = 6.8 Hz, 3H), 1.23-1.40 (m, 12H), 1.46 (quint, *J* = 7.6 Hz, 2H), 1.65 (quint, *J* = 7.6 Hz, 2H), 1.79 (quint, *J* = 7.5 Hz, 2H), 2.65 (t, *J* = 7.7 Hz, 2H), 3.98 (t, *J* = 6.6 Hz, 2H), 6.88 (d, *J* = 8.8 Hz, 2H), 7.27 (d, *J* = 8.2 Hz, 2H), 7.46 (d, *J* = 8.8 Hz, 2H), 7.53 (d, *J* = 8.1 Hz, 2H), 7.56 and 7.59 (AB, *J* = 8.5 Hz, 4H); ^{13}C NMR (125 MHz, $CDCl_3$) δ 14.0, 14.1, 22.5, 22.7, 26.0, 29.19, 29.22, 29.3, 31.2, 31.5, 31.8, 35.6, 68.1, 88.0, 90.0, 114.5, 115.1, 122.2, 126.75, 126.79, 128.9, 131.8, 133.0, 137.7, 140.5, 142.5, 159.2; IR (KBr) ν 2212 (C≡C), 1604, 1510, 1246 cm^{-1}; MALDI-TOF (ANP) *m/z* 452.3 ($[M]^+$) and 453.3 ($[M+1]^+$]. Anal. Calcd for $C_{33}H_{40}O$: C, 87.56; H, 8.91. Found: C, 87.26; H, 8.88.

Preparation of azomethine derivatives 1c. General procedure. A mixture of appropriate aniline **4** (0.15 mmol), 4-octyloxybenzaldehyde[42] (0.15 mmol) and cat. amounts of AcOH in EtOH (2 mL) was refluxed for 1 h. Solvent was evaporated and the crude product was recrystallized repeatedly from hexane.

4-(12-C_5H_{11}-*p*-carboran-1-yl)$C_6H_4N{=}CHC_6H_4OC_8H_{17}$ (1[A]c). White solid, (80% yield): ^{1}H NMR (400 MHz, $CDCl_3$) δ 0.84 (t, *J* = 7.3 Hz, 3H), 0.89 (t, *J* = 6.9 Hz, 3H), 1.05-1.40 (m, 14H), 1.50-4.0 (m, 10H), 1.46 (quint, *J* = 7.4 Hz, 2H), 1.65 (br t, *J* = 8.4 Hz, 2H), 1.80 (quint, *J* = 7.1 Hz, 2H), 4.01 (d, *J* = 6.6 Hz, 2H), 6.94 (d, *J* = 8.9 Hz, 2H), 6.95 (d, *J* = 8.8 Hz, 2H), 7.19 (d, *J* = 8.7 Hz, 2H), 7.78 (d, *J* = 8.7 Hz, 2H), 8.27 (s, 1H); ^{11}B NMR (128 MHz, $CDCl_3$) δ -12.3 (d, *J* = 164 Hz); IR (KBr) ν 2606 (B–H), 1696 (N=C), 1601, 1509, 1256 cm^{-1}; MALDI-TOF (CHCA) *m/z* 520.6–524.6 (max at 523.6, $[MH]^+$). Anal. Calcd for $C_{28}H_{47}B_{10}NO$: C, 64.45; H, 9.08; N, 2.68. Found: C, 64.64; H, 9.19; N, 2.71.

4-(12-C_5H_{11}-*o*-carboran-1-yl)$C_6H_4N{=}CHC_6H_4OC_8H_{17}$ (1[B]c). White solid, (78% yield): ^{1}H NMR (400 MHz, $CDCl_3$) δ 0.73 (t, *J* = 7.3 Hz, 2H), 0.87 (t, *J* = 7.0 Hz, 3H), 0.89 (t, *J* = 6.7 Hz, 3H), 1.22-1.41 (m, 14H), 1.50-4.0 (m, 9H), 1.47 (quint, *J* = 7.1 Hz, 2H), 1.81 (quint, *J* = 7.1 Hz, 2H), 3.90 (br s, 1H), 4.02 (d, *J* = 6.6 Hz, 2H), 6.97 (d, *J* = 8.8 Hz, 2H), 7.09 (d, *J* = 8.7 Hz, 2H), 7.50 (d, *J* = 8.7 Hz, 2H), 7.81 (d, *J* = 8.8 Hz, 2H), 8.31 (s, 1H). Anal. Calcd for $C_{28}H_{47}B_{10}NO$: C, 64.45; H, 9.08; N, 2.68. Found: C, 64.39; H, 9.11; N, 2.65.

4-(4-$C_5H_{11}C_6H_4$)$C_6H_4N{=}CHC_6H_4OC_8H_{17}$ (1[Ph]c). Off-white solid, (80% yield): ^{1}H NMR (400 MHz, $CDCl_3$) δ 0.90 (t, *J* = 7.0 Hz, 3H), 0.91 (t, *J* = 6.8 Hz, 3H), 1.24-1.41 (m, 12H), 1.48 (t, *J* = 7.4 Hz, 2H), 1.66 (quint, *J* = 7.6 Hz, 2H), 1.82 (quint, *J* = 7.1 Hz, 2H), 2.65 (t, *J* = 7.8 Hz, 2H), 4.03 (t, *J* = 6.6 Hz, 2H), 6.98 (d, *J* = 8.8 Hz, 2H), 7.24-7.28 (m, 4H), 7.53 (d, *J* = 8.2 Hz, 2H), 7.61 (d, *J* = 8.5 Hz, 2H), 7.85 (d, *J* = 8.7 Hz, 2H), 8.44 (s, 1H); ^{13}C NMR (125 MHz, $CDCl_3$) δ 14.0, 14.1, 22.6, 22.7, 26.0, 29.16, 29.23, 29.34 31.2, 31.5, 31.8, 35.6, 68.2, 114.7, 121.3, 126.7, 127.6, 128.8, 130.7 (br), 138.0, 138.5, 142.0, 159.4, 162.0; IR (KBr) ν 1606, 1252 cm^{-1}; MALDI-TOF (CHCA) *m/z* 456.4 ($[MH]^+$) and 457.4 ($MH+1]^+$). Anal. Calcd for $C_{32}H_{41}NO$: C, 84.35; H, 9.07; N, 3.07. Found: C, 84.14; H, 9.18; N, 3.11.

Preparation of azobenzene derivatives 1d. General procedure. A mixture of appropriate aniline **4** (0.15 mmol), (*S*)-2-methylbutyl 4-nitrosobenzoate (**5**, 0.15 mmol) and catalytic amounts of AcOH in CH_2Cl_2 (1 mL) was stirred at rt under Ar for 24 h. Reaction with aniline **4[B]** (*o*-carborane) was conducted in AcOH (1 mL). Solvents and AcOH were removed under reduced pressure and the orange crude product was purified on a silica gel plug (hexane/CH_2Cl_2, 3:1) and then recrystallized repeatedly from EtOH.

4-(12-C_5H_{11}-*p*-carboran-1-yl)$C_6H_4N{=}NC_6H_4COOC_5H_{11}$* (1[A]d). Orange solid: ^{1}H NMR (400 MHz, $CDCl_3$) δ 0.85 (t, *J* = 7.2 Hz, 3H), 0.95 (t, *J* = 7.4 Hz, 3H), 1.03 (d, *J* = 6.7 Hz, 3H), 1.06-1.34 (m, 6H), 1.50-3.50 (m, 10H), 1.66 (br t, *J* = 8.5

Hz, 2H), 1.89 (sext, J = 7.1 Hz, 1H), 4.16 (dd, J_1 = 10.7 Hz, J_2 = 6.6 Hz, 1H), 4.24 (dd, J_1 = 10.7 Hz, J_2 = 6.0 Hz, 1H), 7.37 (d, J = 8.8 Hz, 2H), 7.73 (d, J = 8.8 Hz, 2H), 7.90 (d, J = 8.6 Hz, 2H), 8.17 (d, J = 8.6 Hz, 2H); ^{11}B NMR (128 MHz, $CDCl_3$) δ -12.3 (d, J = 164 Hz); IR (KBr) ν 2609 (B–H), 1716 (C=O), 1272 (C–O) cm^{-1}; MALDI-TOF (CHCA) *m/z* 506.5–512.5 (max at 510.5, [MH]$^+$). Anal. Calcd for $C_{25}H_{40}B_{10}N_2O_2$: C, 59.03; H, 7.93; N, 5.51. Found: C, 59.09; H, 7.85; N, 5.44.

4-(12-C_5H_{11}-*o*-carboran-1-yl)C_6H_4N=NC_6H_4COOC_5H_{11}* (1[B]d). Orange solid: ^{1}H NMR (400 MHz, $CDCl_3$) δ 0.75 (br t, J = 7.8 Hz, 2H), 0.88 (t, J = 6.6 Hz, 3H), 0.98 (t, J = 7.4 Hz, 3H), 1.04 (d, J = 6.8 Hz, 3H), 1.22-1.36 (m, 14H), 1.50-4.0 (m, 9H), 1.50-1.62 (m, 2H), 1.81 (sext, J = 7.1 Hz, 1H), 3.98 (br s, 1H), 4.17 (dd, J_1 = 10.7 Hz, J_2 = 6.6 Hz, 1H), 4.25 (dd, J_1 = 10.7 Hz, J_2 = 6.0 Hz, 1H), 7.66 (d, J = 8.8 Hz, 2H), 7.88 (d, J = 8.8 Hz, 2H), 7.95 (d, J = 8.6 Hz, 2H), 8.20 (d, J = 8.6 Hz, 2H); ^{13}C NMR (125 MHz, $CDCl_3$) δ 11.2, 14.0, 16.5, 22.6, 26.3, 29.5, 29.7, 34.3, 35.1, 58.9, 69.3, 67.0, 122.9, 123.2, 128.8, 130.6, 132.8, 136.1, 152.8, 154.8, 166.0; ^{11}B NMR (160 MHz, $CDCl_3$) δ -10.7 (m, 5B), -7.5 (d, J = 146 Hz, 2B), -0.7 (d, J = 148 Hz, 2B), 8.5 (br s, 1B); MALDI-TOF (CHCA) *m/z* 507.5–512.5 (max at 510.5, [MH]$^+$). Anal. Calcd for $C_{25}H_{40}B_{10}N_2O_2$: C, 59.03; H, 7.93; N, 5.51. Found: C, 59.39; H, 7.99; N, 5.50.

4-(4-$C_5H_{11}C_6H_4$)C_6H_4N=NC_6H_4COOC_5H_{11}* (1[Ph]d). Orange solid: ^{1}H NMR (400 MHz, $CDCl_3$) δ 0.92 (t, J = 6.7 Hz, 3H), 0.98 (t, J = 7.5 Hz, 3H), 1.05 (d, J = 6.7 Hz, 3H), 1.20-1.43 (m, 6H), 1.50-1.62 (m, 2H), 1.67 (quint, J = 7.5 Hz, 2H), 1.89 (sext, J = 7.1 Hz, 1H), 2.67 (t, J = 7.7 Hz, 2H), 4.17 (dd, J_1 = 10.7 Hz, J_2 = 6.6 Hz, 1H), 4.25 (dd, J_1 = 10.7 Hz, J_2 = 6.0 Hz, 1H), 7.30 (d, J = 8.1 Hz, 2H), 7.60 (d, J = 8.1 Hz, 2H), 7.76 (d, J = 8.5 Hz, 2H), 7.97 (d, J = 8.4 Hz, 2H), 8.02 (d, J = 8.4 Hz, 2H), 8.20 (d, J = 8.5 Hz, 2H). Anal. Calcd for $C_{29}H_{34}N_2O_2$: C, 78.70; H, 7.74; N, 6.33. Found: C, 78.12; H, 7.69; N, 6.20.

4-(12-(4-$C_5H_{11}OC_6H_4$)-*o*-carboran-1-yl)$CH_2CH_2C_6H_4OC_5H_{11}$ (2[B]f). Styrene derivative[16] **2[B]e** was reduced with H_2 (50 psi) in the presence of Pd/C (10%) in THF. The reaction mixture was filtered, solvent was evaporated and the resulting crude product was passed through a silica gel plug (CH_2Cl_2/hexanes, 1:2) followed by recrystallization (pentane, –78 °C followed by MeOH, –5 °C) giving the desired product as a white solid: ^{1}H NMR (500 MHz, $CDCl_3$) δ 0.91 (t, J = 6.9 Hz, 3H), 0.93 (t, J = 6.9 Hz, 3H), 1.33-1.47 (m, 8H), 1.72-1.80 (m, 4H), 2.50 and 2.73 (A_2X_2, 4H), 3.64 (br s, 1H), 3.91 (t, J = 6.9 Hz, 2H), 3.92 (t, J = 6.9 Hz, 2H), 6.76 (d, J = 8.6 Hz, 2H), 6.82 (d, J = 8.6 Hz, 2H), 7.03 (d, J = 8.6 Hz, 2H), 7.27 (d, J = 8.6 Hz, 2H); ^{13}C NMR (125 MHz, $CDCl_3$) δ 14.0 (2C), 22.5 (2C), 28.20, 28.22, 28.96, 29.02, 34.6, 39.2, 59.9, 67.7, 68.1, 68.6 (br), 113.6, 114.8, 129.1, 130.5, 133.6, 158.0, 158.8; ^{11}B NMR (160 MHz, $CDCl_3$) δ –11.4 (m, 4B), –7.9 (d, J = 158 Hz, 3B), –1.2 (d, J = 151 Hz, 2B), +5.8 (br s, 1B). ESI–HRMS, calcd for $C_{26}H_{44}B_{10}O_2$•Na [M-Na]$^+$ *m/z* 521.4169; found *m/z* 521.4185.

1-(4-Iodophenyl)-12-pentyl-*p*-carborane (3[A], Hal=I). To a solution of bromophenyl derivative[17] **3[A]** (Hal=Br, 100 mg, 0.27 mmol) in THF (10 mL), *n*-BuLi in hexanes (0.33 mmol) was added at –78 °C. After 1 hr solid I_2 was added and the mixture was stirred for 1 hr. The solvent was evaporated, and the residue was passed through a silica gel plug (hexanes). The crude product (90 mg, containing some dehalogenated derivative) was purified by recrystallization (hexane, –10 °C) giving the iodide **3[A], Hal=I** as a white solid: ^{1}H NMR (400 MHz, $CDCl_3$) δ 0.84 (t, J = 7.3 Hz, 3H), 1.05-1.27 (m, 6H), 1.50-3.50 (m, 10H), 1.64 (br t, J = 8.3 Hz, 2H), 6.93 (d, J = 8.7 Hz, 2H), 7.49 (d, J = 8.7 Hz, 2H); ^{11}B NMR (128 MHz, $CDCl_3$) δ -12.4 (d, J = 165 Hz). ESI–HRMS calcd for $C_8H_{14}B_{10}I$ [M–C_5H_{11}]$^+$ *m/z* 347.1078; found *m/z* 347.1053.

1-(4-Aminophenyl)-12-pentyl-*p*-carborane (4[A]). The nitrophenyl derivative **6[A]** (250 mg, 0.75 mmol) in THF (10 mL) was hydrogenated (40 psi) in the presence of 10% Pd/C (25 mg) for 2 hrs. The catalyst was filtered off, the solvent was evaporated, and the resulting crude product was purified by SiO_2 plug (CH_2Cl_2) giving 180 mg (79% yield) of amine **4[A]** as a white solid: mp 85.4-86.0 °C; ^{1}H NMR (400 MHz, $CDCl_3$) δ 0.83 (t, J = 7.3 Hz, 3H), 1.05-1.27 (m, 6H), 1.50-3.50 (m, 10H), 1.63 (br t, J = 8.4 Hz, 2H), 4.00 (br s, 2H), 6.46 (d, J = 8.7 Hz, 2H), 6.97 (d, J = 8.7 Hz, 2H); ^{13}C NMR (125 MHz, $CDCl_3$) δ 13.9, 22.2, 29.2, 31.2, 37.8, 80.4 (br), 81.2 (br), 114.6, 127.2, 128.2, 145.5; ^{11}B NMR (128 MHz, $CDCl_3$) δ -12.4 (d, J = 165 Hz); MALDI-TOF (CHCA) *m/z* 303.4–307.4 (max at 306.4, [M]$^+$). Anal. Calcd for $C_{13}H_{27}B_{10}N$: C, 51.11; H, 8.91; N, 4.59. Found: C, 51.58; H, 9.03; N, 4.63.

(*S*)-2-Methylbutyl 4-nitrosobenzoate (5). Following the general procedure,[27] to a solution of (*S*)-2-methylbutyl 4-aminobenzoate[25,26] (**7**, 310 mg, 1.5 mmol) in CH_2Cl_2 (5 mL), a solution of Oxone® (1.85 g, 3.0 mmol) in water (18 mL) was added under Ar. The mixture was stirred overnight at rt, the organic layer was separated, dried (Na_2SO_4), and solvent was evaporated. The crude product was separated from unreacted starting materials on a short silica gel plug (hexane/CH_2Cl_2, 5:1) to give 100 mg (30% yield) of the nitroso ester **5** as a yellow-green viscous oil, which was used immediately for the next transformation. ^{1}H NMR (400 MHz, $CDCl_3$) δ 0.98 (t, J = 7.5 Hz, 3H), 1.04 (d, J = 6.8 Hz, 3H), 1.25-1.34 (m, 1H), 1.49-1.60 (m, 1H), 1.89 (sext, J = 6.6 Hz, 1H), 4.19 (dd, J_1 = 10.8 Hz, J_2 = 6.6 Hz, 1H), 4.27 (dd, J_1 = 10.8 Hz, J_2 = 6.0 Hz, 1H), 7.94 (d, J = 8.6 Hz, 2H), 8.30 (d, J = 8.6 Hz, 2H).

1-(4-Nitrophenyl)-12-pentyl-*p*-carborane (6[A]). To a solution of *p*-carborane (0.500 g, 3.50 mmol) in dry THF (10 mL), under Ar at –78 °C, *n*-BuLi was added (3.8 mmol). After 0.5 h, the mixture was warmed up to rt and stirred for 0.5 h, then cooled to –78 °C and iodopentane was added (0.45 mL, 3.5 mmol), the mixture was warmed up to rt, and stirred for 1 h. Dry DME (10 mL) was added, the mixture was cooled to –78 °C and *n*-BuLi (3.8 mmol) was added. After 15 min the mixture was allowed to warm to rt, stirred for 0.5 h, cooled to 0 °C and dry CuI (0.73 g, 3.8 mmol) was added. The mixture was stirred at rt for 1 h and pyridine (2.1 mL, 26 mmol) was added followed by 4-iodonitrobenzene (0.872 g, 3.50 mmol) and the mixture was gently refluxed for 20 hr. 10% HCl was added, organic products were extracted (CH_2Cl_2), extracts were dried (Na_2SO_4), solvents were evaporated and the residue was

separated by chromatography (SiO_2, hexane/CH_2Cl_2, 5:1) to give 250 mg (20% yield) of the desired product **6[A]** as the first fraction: mp 83.0-83.5 ^oC; ^1H NMR (400 MHz, $CDCl_3$) δ 0.84 (t, J = 7.3 Hz, 3H), 1.05-1.26 (m, 6H), 1.50-3.40 (m, 10H), 1.66 (br t, J = 8.3 Hz, 2H), 7.38 (d, J = 9.0 Hz, 2H), 8.02 (d, J = 9.0 Hz, 2H); ^{13}C NMR (125 MHz, $CDCl_3$) δ 13.8, 22.2, 29.1, 31.2, 38.0, 78.8 (br), 82.8 (br), 123.2, 128.4, 142.9, 147.6; ^{11}B NMR (128 MHz, $CDCl_3$) δ -12.2 (d, J = 164 Hz); IR (KBr) ν 2614 (B–H), 1598, 1514 (N–O), 1344 (N–O) cm^{-1}. Anal. Calcd for $C_{13}H_{25}B_{10}NO_2$: C, 46.55; H, 7.51; N, 4.18. Found: C, 46.79; H, 7.58; N, 4.27.

Acknowledgment

This work was supported by the NSF grant DMR-1207585.

References

1 R. N. Grimes *Carboranes*; Academic Press: London, 2011.
2 P. Kaszynski In *Boron Science: New Technologies & Applications*; Hosmane, N., Ed.; CRC Press: 2012, p 305-338.
3 P. Kaszynski, A. G. Douglass *J. Organomet. Chem.* 1999, **581**, 28-38.
4 P. Kaszynski, A. Januszko, K. L. Glab *J. Phys. Chem. B* 2014, **118**, 2238-2248.
5 L. Kobr, K. Zhao, Y. Shen, K. Polívková, R. K. Shoemaker, N. A. Clark, J. C. Price, C. T. Rogers, J. Michl *J. Org. Chem.* 2013, **78**, 1768-1777.
6 S. Körbe, P. J. Schreiber, J. Michl *Chem. Rev.* 2006, **106**, 5208-5249.
7 Y. Endo, T. Iijima, Y. Yamakoshi, H. Fukasawa, C. Miyaura, M. Inada, A. Itai *Chem. Biol.* 2001, **8**, 341-355.
8 T. Goto, K. Ohta, S. Suzuki, Y. Ohta, Y. Endo *Bioorg. Med. Chem.* 2005, **13**, 6414-6424.
9 B. T. S. Thirumamagal, X. B. Zhao, A. K. Bandyopadhyaya, S. Narayanasamy, J. Johnsamuel, R. Tiwari, D. W. Golightly, V. Patel, B. T. Jehning, M. V. Backer, R. F. Barth, R. J. Lee, J. M. Backer, W. Tjarks *Bioconjugate Chem.* 2006, **17**, 1141-1150.
10 A. W. Laubengayer, W. R. Rysz *Inorg. Chem.* 1965, **4**, 1513-1514.
11 A. I. Echeistova, Y. K. Syrkin, V. I. Stanko, A. I. Klimova *Russ. J. Struct. Chem.* 1967, **8**, 833-834.
12 P. Kirsch, M. Bremer *Angew. Chem. Int. Ed.* 2000, **39**, 4216-4235.
13 Handbook of Liquid Crystals, 2nd Ed; J. W. Goodby, Collings P. J.; Kato, T.; Tschierske, C.; Gleeson, H.; Raynes, P, Eds.; Wiley-VCH: New York, 2014.
14 B. Ringstrand, P. Kaszynski *J. Mater. Chem.* 2010, **20**, 9613-9615, and references therein.
15 J. Pecyna, B. Ringstrand, R. P. Denicola, H. M. Gray, P. Kaszynski *Liq. Cryst.* 2014, **41**, 1188–1198.
16 A. Jankowiak, P. Kaszynski *Inorg. Chem.* 2014, **53**, 8762−8769.
17 A. G. Douglass, S. Pakhomov, B. Both, Z. Janousek, P. Kaszynski *J. Org. Chem.* 2000, **65**, 1434-1441.
18 K. Czuprynski, A. G. Douglass, P. Kaszynski, W. Drzewinski *Liq. Cryst.* 1999, **26**, 261-269.
19 A. Januszko, K. L. Glab, P. Kaszynski, K. Patel, R. A. Lewis, G. H. Mehl, M. D. Wand *J. Mater. Chem.* 2006, **16**, 3183-3192.
20 R. A. Batey, M. Shen, A. J. Lough *Org. Lett.* 2002, **4**, 1411− 1414.
21 J. Y. Chang, J. H. Baik, C. B. Lee, M. J. Han, S.-K. Hong *J. Am. Chem. Soc.* 1997, **119**, 3197-3198.
22 J. Li, P. Huang *Beils. J. Org. Chem.* 2011, **7**, 426–431.
23 T. Nagamine, A. Januszko, K. Ohta, P. Kaszynski, Y. Endo *Liq. Cryst.* 2008, **35**, 865-884.
24 R. Coult, M. A. Fox, W. R. Gill, P. L. Herbertson, J. A. H. McBride, K. Wade *J. Organomet. Chem.* 1993, **462**, 19-29.
25 J. Newton, H. Walton, H. Colest, P. Hodges *Mol. Cryst. Liq. Cryst.* 1995, 107-125.
26 A. Merlo, A. Gallardo, T. R. Taylor, T. Kroin *Mol. Cryst. Liq. Cryst.* 1994, **250**, 31-39.
27 B. Priewisch, K. Rück-Braun *J. Org. Chem.* 2005, **70**, 2350–2352.
28 For details see the Electronic Supplementary Information.
29 R. Dabrowski, J. Dziaduszek, T. Szczucinski *Mol. Cryst. Liq. Cryst. Lett.* 1984, **102**, 155-160.
30 Z. Raszewski *Liq. Cryst.* 1988, **3**, 307-322.
31 W. Maier, G. Meier *Z. Naturforsch.* 1961, **16A**, 262-267 and 470-477.
32 Urban, S. in Physical Properties of Liquid Crystals: Nematics, D. A. Dunmur, A. Fukuda, and G. R. Luckhurst, Eds; IEE, London, 2001, pp 267-276.
33 L. I. Zakharkin, V. N. Kalinin, E. G. Rys *Bull. Acad. Sci. USSR, Div. Chem. Sci.* 1974, 2543-2545.
34 L. I. Zakharkin, V. N. Kalinin, I. P. Shepilov *Dokl. Akad. Nauk* 1967, **174**, 484EE.
35 P. T. Brain, J. Cowie, D. J. Donohoe, D. Hnyk, D. W. H. Rankin, D. Reed, B. D. Reid, H. E. Robertson, A. J. Welch *Inorg. Chem.* 1996, **35**, 1701-1708.
36 K. Toriyama, S. Sugimori, K. Moriya, D. A. Dunmur, R. Hanson *J. Phys. Chem.* 1996, **100**, 307-315.
37 B. Ringstrand, P. Kaszynski, A. Januszko, V. G. Young, Jr. *J. Mater. Chem.* 2009, **19**, 9204-9212.
38 H. Xianyu, S.-W. Wu, C.-L. Lin *Liq. Cryst.* 2009, **36**, 717-726.
39 M. Mrukiewicz, P. Perkowski, K. Garbat, R. Dabrowski *Liq. Cryst.* 2014, **41**, 1537-1544.
40 Gaussian 09, Revision A.02, M. J. Frisch, G. W. Trucks, H. B. Schlegel, G. E. Scuseria, M. A. Robb, J. R. Cheeseman, G. Scalmani, V. Barone, B. Mennucci, G. A. Petersson, H. Nakatsuji, M. Caricato, X. Li, H. P. Hratchian, A. F. Izmaylov, J. Bloino, G. Zheng, J. L. Sonnenberg, M. Hada, M. Ehara, K. Toyota, R. Fukuda, J. Hasegawa, M. Ishida, T. Nakajima, Y. Honda, O. Kitao, H. Nakai, T. Vreven, J. A. Montgomery, Jr., J. E. Peralta, F. Ogliaro, M. Bearpark, J. J. Heyd, E. Brothers, K. N. Kudin, V. N. Staroverov, R. Kobayashi, J. Normand, K. Raghavachari, A. Rendell, J. C. Burant, S. S. Iyengar, J. Tomasi, M. Cossi, N. Rega, J. M. Millam, M. Klene, J. E. Knox, J. B. Cross, V. Bakken, C. Adamo, J. Jaramillo, R. Gomperts, R. E. Stratmann, O. Yazyev, A. J. Austin, R. Cammi, C. Pomelli, J. W. Ochterski, R. L. Martin, K. Morokuma, V. G. Zakrzewski, G. A. Voth, P. Salvador, J. J. Dannenberg, S. Dapprich, A. D. Daniels, O. Farkas, J. B. Foresman, J. V. Ortiz, J. Cioslowski, and D. J. Fox, Gaussian, Inc., Wallingford CT, 2009.
41 M. Cossi, G. Scalmani, N. Rega, V. Barone *J. Chem. Phys.* 2002, **117**, 43-54 and references therein.
42 A. Januszko, P. Kaszynski, B. Gruner *Inorg. Chem.* 2007, **46**, 6078-6082.

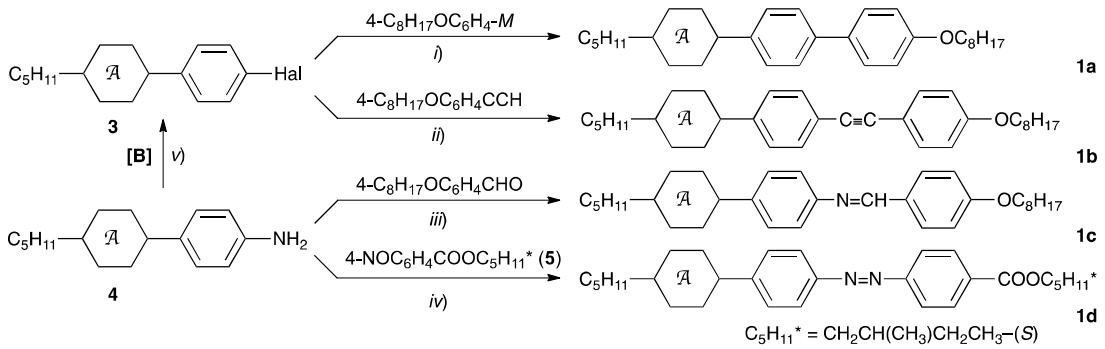

Scheme 1. Synthesis of **1**. Reagents and conditions: *i*) **[A]**: Hal = Br, *M* = $B(OCH_2)_2$, $Pd(PPh_3)_4$, Na_2CO_3, benzene, reflux (ref. [18]); **[B]**: Hal = Br, *M* = ZnCl, $Pd(dba)_2$, $PChx_3$, THF, reflux (ref. [16]); **[Ph]**: Hal = I, *M* = MgBr, $NiBr_2$, THF, reflux (ref. [18]); *ii*) Hal = I, $(i\text{-Pr})_2EtN$, $Pd(PPh_3)_2Cl_2$, CuI, THF, rt; *iii*) EtOH, cat. AcOH, reflux; *iv*) **[A]** and **[C]**: CH_2Cl_2, cat. AcOH, rt; **[B]**: AcOH, rt; *v*) **[B]**, Hal = I: (1) $[NO]^+[PF_6]^-$ and (2) $[Bu_4N]^+[I]^-$, MeCN, 0 °C (ref. [16]).

Table 1. Transition temperatures (°C) for **1**. [a]

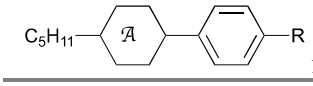

	R	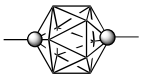 **A**	 **B**	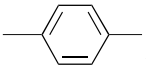 **Ph**
a	$–C_6H_4\text{-}OC_8H_{17}$	Cr 71 (SmA 45) N 149 I [b]	Cr 58 (SmC 38) SmA 121 N 144 I [c]	Cr 97 E 194 SmB 211 SmA 222 I [b]
b	$–C{\equiv}CC_6H_4\text{-}OC_8H_{17}$	Cr 90 N 176 I	Cr 114 SmA 140 N 168 I	Cr 96 Cr 156 B 177 N 206 I
c	$–N{=}CHC_6H_4\text{-}OC_8H_{17}$	Cr 111 N 177 I	Cr 101 SmA 157 N 171 I	Cr 95 (H? 90) G 138 SmF 150 SmI 166 SmC 191 SmA 198 N 214 I
d	$–N{=}NC_6H_4\text{-}COOC_5H_{11}^*$	Cr 94 N* 160 I	Cr 124 N* 151 I	Cr <25 E 115 SmB 136 SmA* 193 I

[a] Enthalpies are reported in the ESI. Cr-crystal, N-nematic, Sm-smectic, soft-crystalline phases B, E and G. [b] Ref [18]. [c] Ref. [16]

Table 2. Transition temperatures (°C) and enthalpies (kJ/mol, in italics) for **2**. [a]

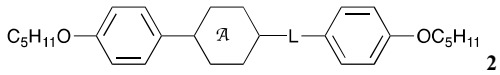

	L	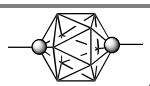 **A**	 **B**	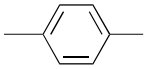 **Ph**
e	–CH=CH–	Cr 124 N 135 I [b]	Cr 121 (N 101) I [c]	Cr 72 X 209 G 254 SmC 258 SmA 281 N 285 I [b]
f	$–CH_2CH_2–$	Cr 94 N 123 I [b]	Cr 81 (N 78) I	Cr 118 B[d] 173 I [b]

[a] Enthalpies are reported in the ESI. Cr-crystal, N-nematic, Sm-smectic, soft-crystalline phases B and G, X-unidentified phase. [b] Ref [23]. [c] Ref. [16]. [d] Previously an E phase was reported.